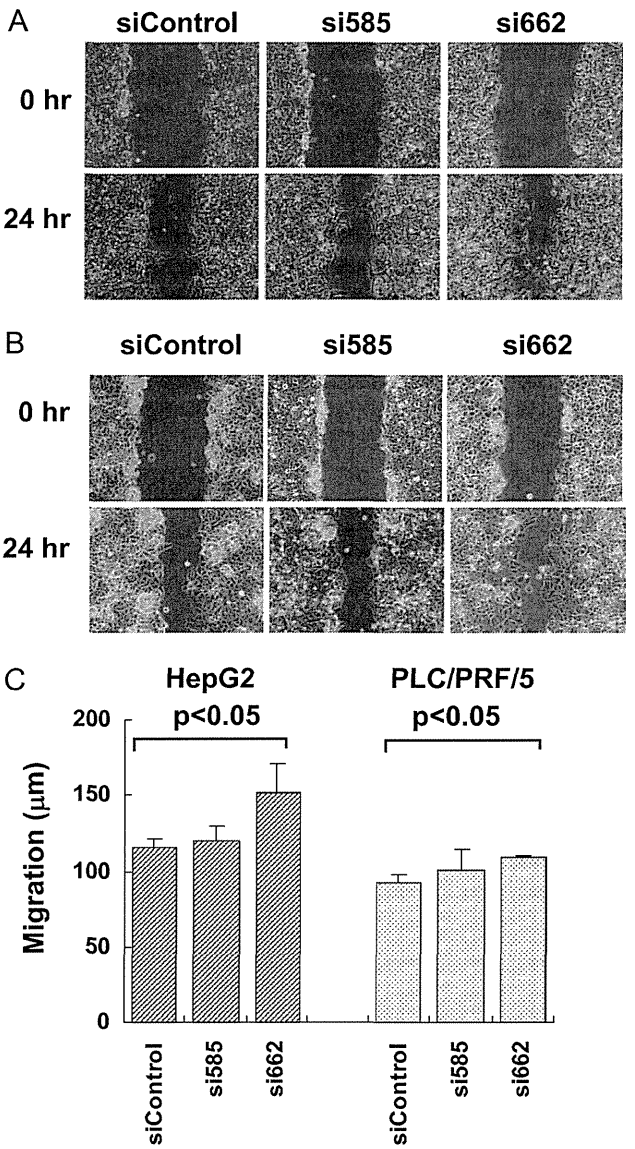

Fig. 5 – Motility of HCC cells after down-regulation of LGR5. Cells transfected with siControl, si585, or si662 were cultured for 2 days. Cell monolayers were scratched and photographed at 24 h. A: HepG2. B: PLC/PRF/5. C: Migration distance.

other non-metastatic [20]. It is quite interesting that KYN-2 and Li7 which express low levels of LGR5 were categorized as highly metastatic, whereas HepG2 and PLC/PRF/5 which express high levels of LGR5 were categorized in the non-metastatic group. Our previous clinicopathological study also showed that overexpression of LGR5 was more frequent in HCC with well to moderate differentiation compared with poorly differentiated HCC, although the difference was not statistically significant [6]. Here, we showed that the level of LGR5 expression in HCC cells affected the morphology of the tumors and their metastatic properties. Our present findings showed similar analogies with the features of clinical HCC regarding LGR5 expression. There is a possibility that high levels of LGR5 expression in HCC be the cause of the typical morphological and biological characteristics of some subclasses of HCC.

We observed similar morphological changes from various kinds of tumor cells by overexpression or down-regulation of LGR5 (unpublished data). One recent report showed that suppression of LGR5 expression in colorectal cancer cells enhanced tumor formation with increased cell motility, while cells overexpressing LGR5 tend to grow in 'colonies' with tight cell-to-cells contact and had reduction in cell motility [10]. Their observations on morphological changes and some other biological functions of LGR5 are mostly in agreement with our results, although the background of cell linage is different. Therefore, we think that our observations from the present study are not specific only to HCC, but are more generally applicable to the certain types of tumors.

Since the ligand of LGR5 has long been unknown, LGR5 has been categorized as an orphan receptor. Recently, R-spondins (Roof plate-specific Spondin, RSPOs) has been reported as ligands of LGR5 and required for sufficient activation of Wnt/β-catenin signaling [11,12,14]. To know whether overexpression of LGR5 affects the expression of RSPOs and potentiate Wnt/β-catenin signaling, we additionally measured expression of R-Spondin 1 (RSPO1) mRNA, and analyzed Wnt/β-catenin signaling level with

TOPflash/FOPflash TCF-luciferase reporter system (Supplementary Fig. 3). The expression of RSPO1 was not dependent on or related to in parallel with LGR5 expression. In HCC cell lines with high levels of LGR5 expression (HepG2), a high expression level of RSPO1 was observed. However, RSPO1 was also highly expressed in KIM 1 with low levels of LGR5. Also in LGR5-overexpressing cell (KY-G1, KY-S1) and empty vector cell (KY-V2, KY-V3), the expression of RSPO1 was not affected. In colorectal cell lines, expression level of RSPO1 was low in high LGR5 expressed cells, LoVo, whereas it was high in low expressed LGR5 cells, HCT116. We found that TOPFLASH/FOPFLASH ratio in LGR5-overexpressing KY-G1 cells was not significantly different from the vector-transfected clone. Furthermore, nuclear accumulation of β-catenin which is usually accompanied with activated Wnt signaling pathway was not detected in the LGR5-overexpressing clone (Fig. 1H). These results suggest that morphological changes and some other properties given from aberrant expression of LGR5 in tumor cells are not likely regulated by augmented Wnt signaling through R-spondin/LGR5 signaling pathway.

In this study we have shown that high levels of LGR5 expression confer cells with some of the properties of stem cells, including sphere formation and enhanced survival. In addition, high levels of LGR5 expression in vivo transformed tumors from a diffuse to a more nodular phenotype and from a metastatic to a less metastatic phenotype. These rather complicated biological roles of LGR5 may explain some of the complexity of human cancers, and further detailed studies of LGR5 would shed light on its biological functions and on the development of effective treatment strategies for cancer.

Disclosure statement

The authors have no conflict of interest.

Acknowledgments

We thank H. Suzuki, Y. Hashimoto and H. Abe for their excellent technical assistance. This work was supported by a Grant-in-Aid for Scientific Research (B) from the Ministry of Education, Culture, Sports, Science and Technology of Japan; and Third Term Comprehensive 10-Years Strategy for Cancer Control from the Ministry of Health, Labor and Welfare of Japan to M.S.

Appendix A. Supporting information

Supplementary data associated with this article can be found in the online version at http://dx.doi.org/10.1016/j.yexcr.2012.10.011.

REFERENCES

[1] H. Morita, S. Mazerbourg, D.M. Bouley, C.W. Luo, K. Kawamura, Y. Kuwabara, H. Baribault, H. Tian, A.J. Hsueh, Neonatal lethality of LGR5 null mice is associated with ankyloglossia and gastrointestinal distension, Mol. Cell. Biol. 24 (2004) 9736–9743.

[2] M.I. Garcia, M. Ghiani, A. Lefort, F. Libert, S. Strollo, G. Vassart, LGR5 deficiency deregulates Wnt signaling and leads to precocious Paneth cell differentiation in the fetal intestine, Dev. Biol. 331 (2009) 58–67.

[3] N. Barker, J.H. van Es, J. Kuipers, P. Kujala, M. van den Born, M. Cozijnsen, A. Haegebarth, J. Korving, H. Begthel, P.J. Peters, H. Clevers, Identification of stem cells in small intestine and colon by marker gene Lgr5, Nature 449 (2007) 1003–1007.

[4] N. Barker, R.A. Ridgway, J.H. van Es, M. van de Wetering, H. Begthel, M. van den Born, E. Danenberg, A.R. Clarke, O.J. Sansom, H. Clevers, Crypt stem cells as the cells-of-origin of intestinal cancer, Nature 457 (2009) 608–611.

[5] V. Jaks, N. Barker, M. Kasper, J.H. van Es, H.J. Snippert, H. Clevers, R. Toftgard, Lgr5 marks cycling, yet long-lived, hair follicle stem cells, Nat. Genet. 40 (2008) 1291–1299.

[6] Y. Yamamoto, M. Sakamoto, G. Fujii, H. Tsuiji, K. Kenetaka, M. Asaka, S. Hirohashi, Overexpression of orphan G-protein-coupled receptor, Gpr49, in human hepatocellular carcinomas with beta-catenin mutations, Hepatology 37 (2003) 528–533.

[7] K. Tanese, M. Fukuma, T. Yamada, T. Mori, T. Yoshikawa, W. Watanabe, A. Ishiko, M. Amagai, T. Nishikawa, M. Sakamoto, G-protein-coupled receptor GPR49 is up-regulated in basal cell carcinoma and promotes cell proliferation and tumor formation, Am. J. Pathol. 173 (2008) 835–843.

[8] T. McClanahan, S. Koseoglu, K. Smith, J. Grein, E. Gustafson, S. Black, P. Kirschmeier, A.A. Samatar, Identification of overexpression of orphan G protein-coupled receptor GPR49 in human colon and ovarian primary tumors, Cancer Biol. Ther. 5 (2006) 419–426.

[9] H. Uchida, K. Yamazaki, M. Fukuma, T. Yamada, T. Hayashida, H. Hasegawa, M. Kitajima, Y. Kitagawa, M. Sakamoto, Overexpression of leucine-rich repeat-containing G protein-coupled receptor 5 in colorectal cancer. Cancer Science 101 (2010) 1731–1737.

[10] F. Walker, H.H. Zhang, A. Odorizzi, A.W. Burgess, LGR5 is a negative regulator of tumourigenicity, antagonizes Wnt signalling and regulates cell adhesion in colorectal cancer cell lines. PloS one 6 (2011) e22733.

[11] W. de Lau, N. Barker, T.Y. Low, B.K. Koo, V.S. Li, H. Teunissen, P. Kujala, A. Haegebarth, P.J. Peters, M. van de Wetering, D.E. Stange, J.E. van Es, D. Guardavaccaro, R.B. Schasfoort, Y. Mohri, K. Nishimori, S. Mohammed, A.J. Heck, H. Clevers, Lgr5 homologues associate with Wnt receptors and mediate R-spondin signalling. Nature 476 (2011) 293–297.

[12] K.S. Carmon, Q. Lin, X. Gong, A. Thomas, Q. Liu, LGR5 interacts and cointernalizes with Wnt receptors to modulate Wnt/beta-catenin signaling. Molecular and Cellular Biology 32 (2012) 2054–2064.

[13] Y. Komiya, R. Habas, Wnt signal transduction pathways, Organogenesis 4 (2008) 68–75.

[14] A. Glinka, C. Dolde, N. Kirsch, Y.L. Huang, O. Kazanskaya, D. Ingelfinger, M. Boutros, C.M. Cruciat, C. Niehrs, LGR4 and LGR5 are R-spondin receptors mediating Wnt/beta-catenin and Wnt/PCP signalling. EMBO Reports 12 (2011) 1055–1061.

[15] T. Reya, S.J. Morrison, M.F. Clarke, I.L. Weissman, Stem cells, cancer, and cancer stem cells, Nature 414 (2001) 105–111.

[16] R. Pardal, M.F. Clarke, S.J. Morrison, Applying the principles of stem-cell biology to cancer, Nature Rev. 3 (2003) 895–902.

[17] N. Sato, L. Meijer, L. Skaltsounis, P. Greengard, A.H. Brivanlou, Maintenance of pluripotency in human and mouse embryonic stem cells through activation of Wnt signaling by a pharmacological GSK-3-specific inhibitor, Nature Med. 10 (2004) 55–63.

[18] X. Gong, K.S. Carmon, Q. Lin, A. Thomas, J. Yi, Q. Liu, LGR6 is a high affinity receptor of R-spondins and potentially functions as a tumor suppressor. PloS one 7 (2012) e37137.

[19] Y. Mimori-Kiyosue, C. Matsui, H. Sasaki, S. Tsukita, Adenomatous polyposis coli (APC) protein regulates epithelial cell migration and morphogenesis via PDZ domain-based interactions with plasma membranes, Genes Cells 12 (2007) 219–233.

[20] M. Chuma, M. Sakamoto, J. Yasuda, G. Fujii, K. Nakanishi, A. Tsuchiya, T. Ohta, M. Asaka, S. Hirohashi, Overexpression of cortactin is involved in motility and metastasis of hepatocellular carcinoma, J. hepatology 41 (2004) 629–636.

Research Article

EASL EUROPEAN ASSOCIATION FOR THE STUDY OF THE LIVER | JOURNAL OF HEPATOLOGY

Diacylglycerol kinase alpha enhances hepatocellular carcinoma progression by activation of Ras–Raf–MEK–ERK pathway

Kazuki Takeishi[1], Akinobu Taketomi[1,*], Ken Shirabe[1], Takeo Toshima[1], Takashi Motomura[1], Toru Ikegami[1], Tomoharu Yoshizumi[1], Fumio Sakane[2], Yoshihiko Maehara[1]

[1]*Department of Surgery and Science, Graduate School of Medical Sciences, Kyushu University, Fukuoka, Japan;* [2]*Department of Chemistry, Graduate School of Science, Chiba University, Chiba, Japan*

Background & Aims: Diacylglycerol kinases (DGKs) were recently recognized as key regulators in cell signaling pathways. We investigated whether DGKα is involved in human hepatocellular carcinoma (HCC) progression.

Methods: We silenced or overexpressed DGKα in HCC cells and assessed its effect on tumor progression. DGKα expression in 95 surgical samples was analyzed by immunohistochemistry, and the expression status of each sample was correlated with clinicopathological features.

Results: DGKα was detected in various HCC cell lines but at very low levels in the normal liver. Knockdown of DGKα significantly suppressed cell proliferation and invasion. Overexpression of wild type (WT) DGKα, but not its kinase-dead (KD) mutant, significantly enhanced cell proliferation. DGKα knockdown impaired MEK and ERK phosphorylation, but did not inhibit Ras activation in HCC cells. In a xenograft model, WT DGKα overexpression significantly enhanced tumor growth compared to the control, but KD DGKα mutant had no effect. Immunohistochemical studies showed that DGKα was expressed in cancerous tissue, but not in adjacent non-cancerous hepatocytes. High DGKα expression (≥20%) was associated with high Ki67 expression (p <0.05) and a high rate of HCC recurrence (p = 0.033) following surgery. In multivariate analyses, high DGKα expression was an independent factor for determining HCC recurrence after surgery.

Conclusions: DGKα is involved in HCC progression by activation of the MAPK pathway. DGKα could be a novel target for HCC therapeutics as well as a prognostic marker.

Keywords: Liver cancer; Diacylglycerol; Phosphatidic acid; Diacylglycerol kinase; MAP kinase.

Received 21 November 2011; received in revised form 2 February 2012; accepted 13 February 2012; available online 14 March 2012

* Corresponding author. Address: Department of Surgery and Science, Graduate School of Medical Sciences, Kyushu University, 3-1-1, Maidashi, Higashi-ku, Fukuoka 812-8582, Japan. Tel.: +81 92 642 5466; fax: +81 92 642 5482.

E-mail address: taketomi@surg2.med.kyushu-u.ac.jp (A. Taketomi).

Abbreviations: HCC, hepatocellular carcinoma; MAPK, mitogen-activated protein kinase; DGK, diacylglycerol kinase; DG, diacylglycerol; PA, phosphatidic acid; siRNA, small interfering RNA; ERK, extracellular signal-regulated kinase; MEK, MAPK/ERK kinase; HGF, hepatocyte growth factor; WT, wild type; KD, kinase dead; FACS, fluorescence activated cell sorting.

Introduction

Hepatocellular carcinoma (HCC) is one of the most common solid tumors worldwide and its incidence is continuing to increase [1,2]. The main therapies for HCC are curative strategies such as liver resection or liver transplantation [3,4]. As these treatments are only viable for patients with preserved liver function, or for those with access to a donor organ, there are many patients with incurable HCC [5,6]. In addition, the long-term outcome after these therapies remains unsatisfactory because of high recurrence rates [3,5]. Therefore, new novel therapeutic strategies for HCC are required.

HCC is associated with increased expression and activity of mitogen-activated protein kinase (MAPK) signaling intermediates [7,8]. Activated Ras induces the Raf–MAPK/ERK kinase (MEK)-extracellular signal-regulated kinase (ERK) cascade, which regulates various cellular responses, including proliferation, survival, and migration [7–9].

Diacylglycerol kinase (DGK) catalyzes the phosphorylation of diacylglycerol (DG) to generate phosphatidic acid (PA) [10–14]. DG and PA are recognized as important second messengers, and play key roles in signal transduction and cellular function [11–14]. DGKs have critical tasks in signal transmission from many receptors, and modulate diverse cellular processes, regulating both DG and PA levels. To date, 10 mammalian DGK isozymes (α–θ) have been identified, and all have the catalytic region in common [10–14]. DGKα is subdivided into the type I group due to its calcium-binding EF-hand motifs and recoverin homology domain [15–17]. This enzyme was first identified in T lymphocytes/thymus and enhances interleukin 2-induced T cell proliferation [15,18,19]. Another report demonstrated that DGKα overexpression resulted in a defect in T cell receptor signaling characteristic of anergy [20,21]. These reports collectively suggest that DGKα has various biological roles.

Here, we found that DGKα was expressed in several human liver cancer cell lines, but only at very low levels in the normal liver. In order to identify HCC-specific functions of DGKα, this isoform was downregulated and then conversely overexpressed in two types of HCC cell lines by transfecting small interfering RNA (siRNA) and DGKα expression plasmids, respectively. Interestingly, this study clarified that DGKα positively regulated proliferation and invasion of human HCC cells through activation of MAPK signaling. Furthermore, immunohistochemical studies

Cancer

of surgical samples suggested that high DGKα expression was associated with HCC recurrence after surgery.

Materials and methods

Cell culture

Human HCC cell lines, HuH7, PLC/PRF/5, HLE, and Hep3B, were cultured in Dulbecco's modified Eagle's medium supplemented with 10% fetal bovine serum, 100 IU/ml penicillin, and 100 mg/ml streptomycin sulfate (Life Technologies, Inc., Carlsbad, CA). All cells were maintained at 37 °C in 5% CO_2.

Antibodies and reagents

Anti-pig DGKα polyclonal antibodies (cross-reactive with human DGKα) were prepared as described previously [22]. Other antibodies were obtained from commercial sources as follows: anti-Ras antibody (Upstate Biotechnology, Inc., Waltham, MA), anti-ERK1/2, anti-phosphorylated-ERK1/2 (Thr-202/Tyr-204), anti-MEK1/2, and anti-phosphorylated-MEK1/2 (Ser-217/221) antibodies (Cell Signaling Technology Inc., Beverly, MA), anti-actin, anti-GAPDH and anti-cyclin D1 monoclonal antibodies (Santa Cruz Biotechnology Inc., Santa Cruz, CA), anti-Ki67 monoclonal antibodies (Dako, Tokyo, Japan) and anti-GFP monoclonal antibodies (Nacalai Tesque, Kyoto, Japan). Recombinant human hepatocyte growth factor (HGF) was purchased from Peprotech (Rocky Hill, NJ).

Human tissue samples

Samples from 95 patients who had undergone liver resection for HCC without preoperative treatment at the Department of Surgery and Science, Kyushu University Hospital, between January 1998 and December 2002 were analyzed by immunohistochemistry. Patients' clinical features are shown in Table 1. Histological diagnoses of the tumors were based on the General Rules for the Clinical and Pathological Study of Primary Liver Cancer by the Liver Cancer Study Group of Japan [23]. Written, informed consent was obtained from each patient for the study of tissue excised from surgical specimens. The Kyushu University Medical human investigation committee gave approval for this study.

Plasmids

cDNAs encoding wild type (WT) DGKα and kinase-dead (KD) DGKα were generated as previously described [15,24] and were subcloned into pEGFP-C3 and pcDNA 1.1 vectors. Cells were transiently transfected using Lipofectamine LTX (Invitrogen, Carlsbad, CA), according to the manufacturer's instructions. To generate stable cell lines that permanently expressed exogenous GFP alone, GFP–DGKα WT or GFP–DGKα KD, 1 μg of linearized DNA was transfected, and cells were selected for neomycin resistance using 2 mg/ml of G418. Individual clones were isolated and tested for expression of GFP by Western blot analysis.

Immunohistochemistry

Paraffin sections of samples were deparaffinized. Heat-induced epitope retrieval was performed in 0.1 M NaOH citrate buffer (pH 7.0), and the samples were heated in an autoclave. Immunoreactivity was independently graded by two liver pathologists. At least 1000 cancer cells in five high-power fields were counted.

RNA interference

To silence the expression of human DGKα, the following oligonucleotides (Invitrogen, Carlsbad, CA) were used: *DGKα1* sense; 5′-CGAGGAUGGCGAGAUGGCUAAAUAU-3′, and *DGKα2* sense; 5′-GCGAGUCAAGCAUUGGUCUUGGCAA-3′. As a negative control, scrambled siRNA was used. The annealed oligonucleotide duplex siRNA (10 nM) was transfected into cells using Lipofectamine RNAi max (Invitrogen, Carlsbad, CA) according to the manufacturer's instructions.

Cell proliferation assays

PLC/PRF/5 and HuH7 cells were seeded in 60 mm dishes at a density of 2×10^5. After days 0, 2, 4, 6, and 8 of transfection with plasmid or siRNA, cells were trypsinized. Cells excluding trypan blue were counted using a hemocytometer.

Invasion assays

Invasion analyses were performed as described previously [25]. Invasive indexes were calculated using the following formula: Invasion index (%) = (number of cells that invaded through Matrigel insert membrane)/(number of cells that migrated through control insert membrane). Each experiment was performed in triplicate wells and repeated three times.

Protein extraction and Western blot analysis

Protein extraction and Western blot analysis were performed as described [26]. To measure the relative density of immunoreactive bands, images were scanned and analyzed by Image J software (National Institute of Health., Bethesda, MD).

Affinity precipitation of activated Ras

Cells were lysed in lysis buffer (50 mM Tris pH 7.5, 10 mM $MgCl_2$, 0.5 M NaCl, and 2% Igepal). The supernatant was incubated with 10 μl of Raf–Ras–binding domain (RBD)–GST beads (Cytoskeleton Inc., Denver, CO), which selectively interacted with active GTP–bound Ras. The beads were washed three times with wash buffer (25 mM Tris pH 7.5, 30 mM $MgCl_2$, 40 mM NaCl) containing 5 mM $MgCl_2$, and then boiled in SDS sample buffer. Ras associated with Raf–RBD–GST and total Ras in cell lysates were detected with anti-Ras antibody using Western blot analysis.

Fluorescence-activated cell sorting (FACS)

HCC cells were transfected with siRNA. After 48 h, cells were incubated with 40 ng/ml of HGF for 48 h. Adherent and floating cells were then pooled and washed with ice-cold PBS. Cells were fixed with ice-cold 70% ethanol and labeled with PI, followed by FACS. G1, S and G2/M populations were quantified using FACS Scan Cell Sorter (BD Biosciences, Tokyo, Japan) using FlowJo software (Tree Star, Ashland, OR).

Xenograft model

BALB/c male nude mice (Charles River, Yokohama, Japan) were maintained according to the Institutional Animal Care and Use Committee of the Kyushu University Graduate School of Medical Sciences. Tumors were generated by subcutaneously injecting 5×10^6 PLC/PRF/5 cells stably expressing endogenous GFP alone, GFP–DGKα WT, or GFP–DGKα KD. Tumor dimensions were measured once a week, and tumor volume was calculated using the following formula: tumor volume (mm^3) = (the largest diameters)/2 × (the smallest diameters)/2 [27]. Mice were euthanized when tumors reached 10% of their body weight or when the skin overlying tumors became ulcerated.

Statistical analysis

JMP 8J Version (SAS Institute, Cary, NC) was used for all analyses. All experiments were independently performed three times in triplicate. Comparisons between groups were made using Wilcoxon test with continuous variables and Fisher's exact test for comparisons of proportions. Survival curves were estimated using the Kaplan–Meier method, and the differences in survival rates between groups were compared by the log-rank test. Multivariate analysis was performed using Cox's proportional hazard regression model to evaluate the independent factors predictive of patients' survival. By multivariate analysis, we examined the following six clinicopathological factors, which were significant factors in the univariate analysis: (1) positive for hepatitis C virus antibody; (2) indocyanine green 15-min retention test (>15% *vs.* ⩽15%); (3) positive for intrahepatic metastasis; (4) DGKα (high *vs.* low expression); (5) liver cirrhosis, (6) AFP (>40 *vs.* ⩽40). Data are expressed as mean ± standard deviation. p Values of <0.05 were considered to be significant.

Table 1. Relationship between DGKα expression and clinicopathological factors.

Factors	All patients	DGKα expression		*p* value
		Low	High	
	(n = 95)	(n = 78)	(n = 17)	
Gender, male (%)	80	78	88	0.51
Age (yr)	63 ± 9	64 ± 10	61 ± 9	0.41
HBsAg positive (%)	21	19	29	0.34
Anti-HCV Ab positive (%)	61	60	65	0.79
Albumin (g/dl)	4.0 ± 0.4	4.0 ± 0.4	4.0 ± 0.5	0.59
Total bilirubin (mg/dl)	0.9 ± 0.3	0.9 ± 0.3	0.9 ± 0.3	0.60
AST (IU/L)	51 ± 28	52 ± 29	45 ± 22	0.38
ALT (IU/L)	54 ± 43	53 ± 34	64 ± 73	0.34
ICG-R15 (%)	16 ± 9	16 ± 8	15 ± 8	0.49
Platelet (x 10^3/μl)	69 ± 114	69 ± 124	78 ± 84	0.77
Child-Pugh A/B, C (%)	84/16	84/16	88/12	0.49
AFP (ng/ml)	7050 (1.7-41,000)	9000 (1.7-5600)	607 (5.3-41,000)	1.00
Cirrhosis (%)	31	31	24	0.77
Tumor size (cm)	4.2 ± 3.1	4.2 ± 3.2	4.7 ± 2.6	0.54
Stage I, II/III, IV (%)*	42/58	45/55	24/76	0.17
Differentiation: well, moderately/poorly (%)	70/30	68/32	76/24	0.57
Portal vein invasion (%)	47	46	59	0.43
Intrahepatic metastasis (%)	23	19	41	0.06

DGKα, diacylglycerol kinase α; HBsAg, hepatitis B surface antigen; anti-HCV Ab, anti- hepatitis C virus antibody; ALT, alanine aminotransferase; AST, aspartate aminotransferase; ICG-R15, indocyanine green 15-min retention test; AFP, α-fetoprotein.
*Tumor staging was defined according to the Liver Cancer Study Group of Japan [23].

Results

DGKα is upregulated in HCC

DGKα expression in HCC cell lines was examined by Western blotting. Fig. 1A shows that DGKα was expressed in all HCC cell lines, but was almost insignificant in primary cultured normal hepatocytes prepared from surgically resected specimens of patients with liver metastasis, indicating that DGKα is expressed in HCC and the expression is stronger than in non-cancerous hepatocytes.

Knockdown of DGKα suppresses HCC cell proliferation and invasion

To determine the role of DGKα in HCC, DGKα expression was suppressed by siRNA in two HCC cell lines, PLC/PRF/5 and HuH7. We used these cell lines for analysis because they have different features: PLC/PRF/5 cells are positive for hepatitis B surface antigen and represent poorly differentiated HCC, whereas HuH7 cells are negative for hepatitis B surface antigen and represent well differentiated HCC [28,29]. *DGKα*-specific siRNA successfully silenced the expression of DGKα 48 h after transfection in PLC/PRF/5 (Supplementary Fig. 1A) and HuH7 (data not shown) cells. As previous reports demonstrated that DGKα positively regulates T cell proliferation and vascular endothelial cell invasion [18,30], the proliferation and invasion of *DGKα*-silenced HCC cells were compared to those of wild type cells. Knockdown of DGKα expression significantly inhibited HCC cell proliferation (Fig. 1B and C). FACS analysis also showed that loss of DGKα increased G1 phase and reduced G2/S phase of HCC cells (Fig. 1D). Furthermore, DGKα knockdown decreased cyclin D1 expression, indicating that it may be a target of DGKα (Fig. 1E). Next, the invasive activity of DGKα in HCC cells was investigated. Silencing of *DGKα* reduced cell invasion (Fig. 1F). These results suggest that DGKα plays a key role in promoting HCC cell proliferation and invasion.

Overexpression of DGKα catalytic activity promotes HCC cell proliferation

In the reverse experiment, we overexpressed DGKα in HCC cells. Exogenous GFP alone, GFP–DGKα WT, and GFP–DGKα KD proteins were expressed by transfecting plasmids (Supplementary Fig. 1B); exogenous WT DGKα expression was about five times that of endogenous DGKα in HCC cells (data not shown). WT DGKα overexpression significantly enhanced HCC cell proliferation (Fig. 2A and B). Although the expression level of KD DGKα was almost the same as that of WT DGKα (Supplementary Fig. 1B), this mutant failed to affect the extent of cell proliferation (Fig. 2A and B), indicating that DGKα catalytic activity is required to promote cell proliferation.

DGKα activates the Ras–Raf–MEK–ERK pathway in HCC cells

To elucidate the mechanism by which DGKα enhances cell proliferation and invasion, HGF-induced ERK1/2 activation in *DGKα*-silenced HCC cells was subsequently examined. It has been reported that activation of the Ras–Raf–MEK–ERK pathway is ubiquitous in human HCC, and its activation is associated with tumor growth and invasion [8,31]. In PLC/PRF/5 and HuH7, DGKα depletion significantly inhibited the increase in ERK1/2 phos-

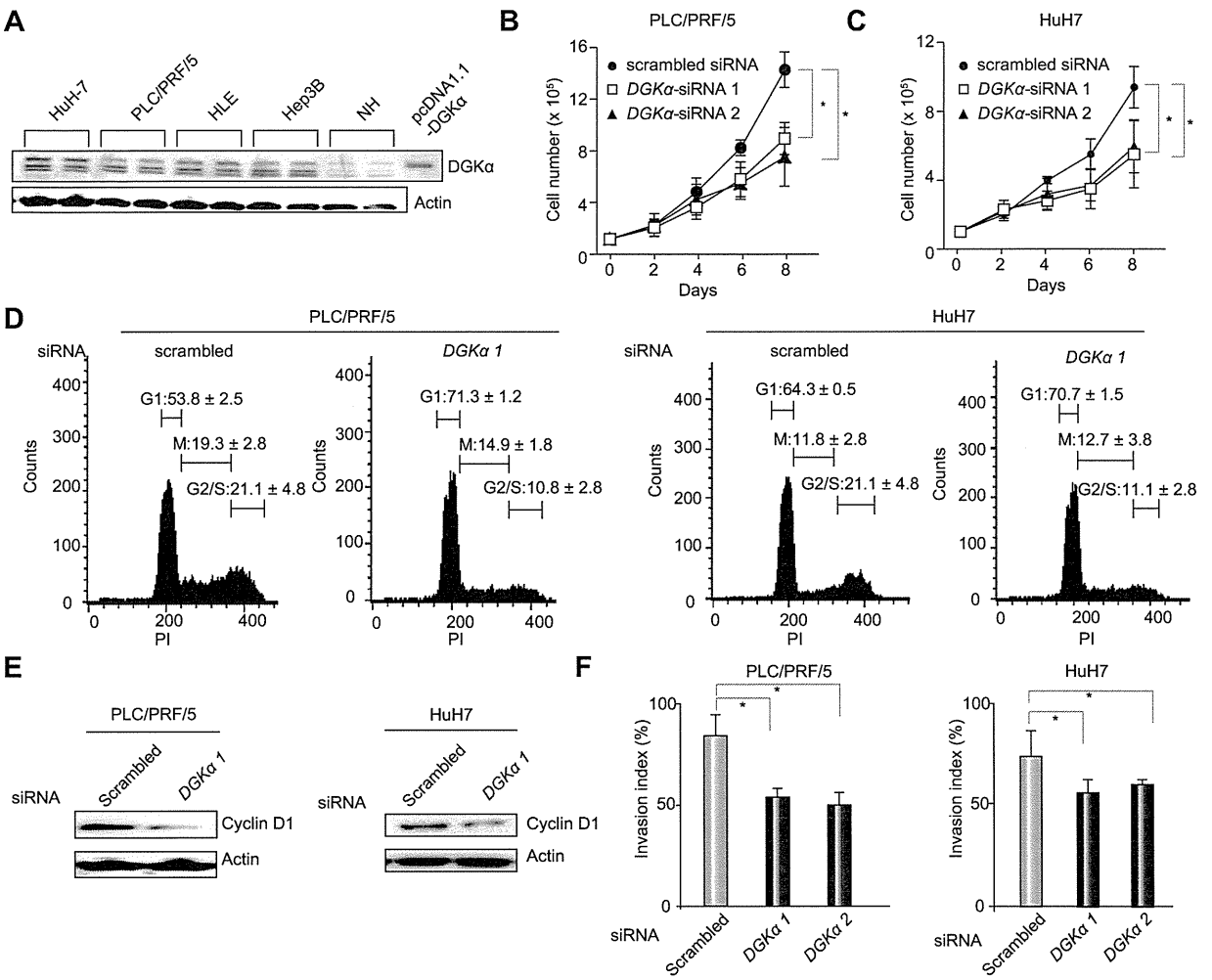

Fig. 1. DGKα expression in HCC cell lines and inhibition of HCC cell proliferation and invasion caused by silencing of *DGKα*. (A) DGKα expression in human HCC cells and normal hepatocytes (NH) was analyzed. At the indicated times after transfections, (B) PLC/PRF/5 and (C) HuH7 cells were counted. (D) Histograms show DNA content (*x*-axis) plotted *vs.* relative cell number (*y*-axis). (E) After DGKα knockdown, cyclin D1 expression was analyzed. (F) Following DGKα knockdown, cancer cells that had migrated through the membrane to the lower surface were counted. Data shown are representative of at least three experiments. Asterisks (*) indicate statistical significance between DGKα-specific and scrambled siRNA.

phorylation, following stimulation with HGF for 5 min, by 90% and 50%, respectively (Fig. 2C and D and Supplementary Fig. 2A and D). The effect of *DGKα* silencing on HGF-induced phosphorylation of kinases upstream of ERK1/2, MEK1/2 was subsequently examined. In PLC/PRF/5 and HuH7, depletion of DGKα also inhibited MEK1/2 phosphorylation, following 5 min of HGF stimulation, by 55% and 50%, respectively (Fig. 2C and D and Supplementary Fig. 2B and E). In contrast, DGKα depletion did not impair the activity of Ras following 5 and 30 min of HGF stimulation, but significantly activated Ras compared with the control, following HGF stimulation for 60 min in PLC/PRF/5 and HuH7, by 40% and 50%, respectively (Fig. 2C and D and Supplementary Fig. 2C and F). Collectively, these results suggest that DGKα plays an important role in activation of HGF-induced MAPK pathways, and that the target component of DGKα is upstream of MEK and downstream of Ras.

DGKα induces tumor growth in xenograft models

We generated stable cell lines expressing either exogenous GFP alone, GFP–DGKα WT or GFP–DGKα KD. To investigate whether DGKα enhanced tumor growth *in vivo*, xenograft models were generated by subcutaneous injection of these stable transformants. Successful overexpression in xenograft models was confirmed by Western blotting (Fig. 3C). Overexpression of WT DGKα promoted significant subcutaneous tumor growth compared to that of GFP alone (Fig. 3A). There were no significant differences in tumor growth between GFP alone and KD DGKα (Fig. 3B). Overexpression of WT DGKα, but not KD DGKα, activated MEK and ERK, and induced cyclin D1 upregulation (Fig. 3C). Ki67 is a nuclear protein expressed in all proliferating cells [32]. To compare the rate of cell proliferation, subcutaneous tumors were immunostained with anti-Ki67 antibody 42 days

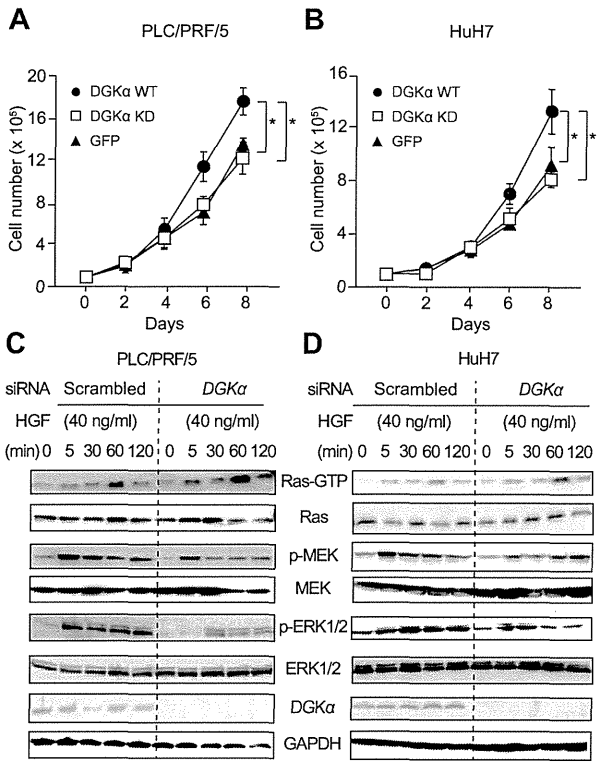

Fig. 2. Effect of DGKα overexpression on HCC cell proliferation and impaired activation of MAPK signaling in DGKα-silenced HCC cells following HGF stimulation. At the indicated times after transfection, (A) PLC/PRF/7 and (B) HuH7 cells were counted. Data shown are representative of at least three experiments. Asterisks (*) indicate statistical significance between cells transfected with WT DGKα and GFP alone or KD DGKα. (C and D) Ras-GTP precipitated with GST-Raf-RBD and total Ras, phosphorylated-MEK1/2 (p-MEK1/2), total MEK1/2, total ERK, phosphorylated-ERK1/2 (p-ERK1/2) and DGKα in cell lysates were detected by Western blotting. Downregulation of p-MEK1/2 and p-ERK1/2, but not Ras-GTP in DGKα-silenced HCC cells at all times after HGF stimulation.

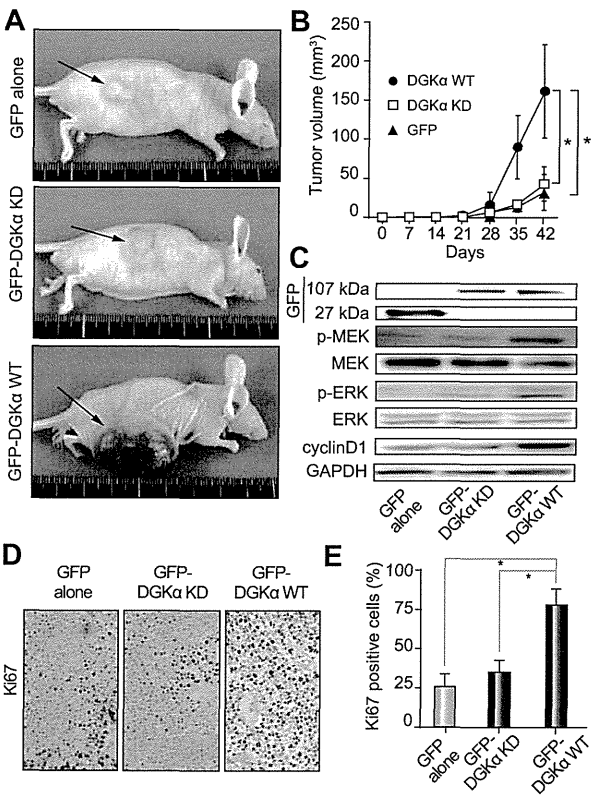

Fig. 3. Effect of DGKα on *in vivo* growth of PLC/PRF/5 cell-derived tumors. GFP alone, GFP-WT DGKα, or GFP-KD DGKα stable cell lines were injected subcutaneously into nude mice. (A) Forty-two days after injection, tumors were photographed. (B) Tumor growth was monitored for 42 days. (C) Phosphorylated-MEK (p-MEK) 1/2, total MEK1/2, phosphorylated-ERK (p-ERK) 1/2, total ERK, and cyclin D1 were detected. (D) Tumor samples were subjected to immunohistochemistry using Ki67 (400 × magnification). (E) Cell numbers positive for Ki67 are shown as mean ± S.D. Asterisks (*) indicate the statistical significance between tumors overexpressing WT DGKα and tumors overexpressing GFP alone or KD DGKα.

after injection with stably-expressing tumor cell lines. Tumors with overexpressed WT DGKα had significantly higher levels of Ki67 than those expressing GFP alone or KD DGKα (77% *vs.* 27% or 33%, respectively; $p < 0.05$) (Fig. 3D and E). DGKα activated MAPK signaling, and positively regulated cell proliferation in HCC *in vivo* models, which correlated with the results observed in *in vitro* models.

High DGKα expression in HCC is a risk factor for recurrence after hepatectomy

Western blot analysis showed that DGKα was detected at higher levels in cancerous tissues from surgical samples than in adjacent non-cancerous tissues (Fig. 4A). DGKα expression was immunohistochemically examined in 95 HCC resected tissue samples. Normal bile duct cells showed specific DGKα expression and were used as the internal positive control in all cases. DGKα immunoreactivity in cancer cells was observed in the cytoplasm and partially in the nucleus; however, hepatocytes from matched adjacent non-cancerous tissues were negative for DGKα immunoreactivity (Fig. 4B). The 95 cases were divided into two groups: a high DGKα expression group (n = 17) with ⩾20% of cancer cells staining positively for DGKα, and a low DGKα expression group with <20% cancer cells staining positively for DGKα. Table 1 shows a comparison of the clinicopathological factors between the high and low DGKα expression groups. There were no significant differences in clinicopathological factors between the two groups. Ki67 was also detected in the nuclei of cancer cells but not in corresponding non-cancerous tissues (Fig. 4B). The high DGKα expression group had significantly more positive Ki67 staining than the low DGKα expression group (11% *vs.* 3.7%; $p < 0.05$) (Fig. 4C). Phosphorylated-ERK1/2 expression was also detected in cancer cells but not in adjacent non-cancerous tissues (Fig. 4B); however, it could not be compared with DGKα expression by immunohistochemistry because it was expressed at low levels (12/95; 12%). Disease-free survival after hepatectomy was compared between the two groups; the disease-free survival rates of the low DGKα-expressing patients (59% at 3-year and 47% at 5-year) was significantly better than that of high-expressing patients (48% at 3-year and 18% at 5-year) ($p = 0.033$; Fig. 4D).

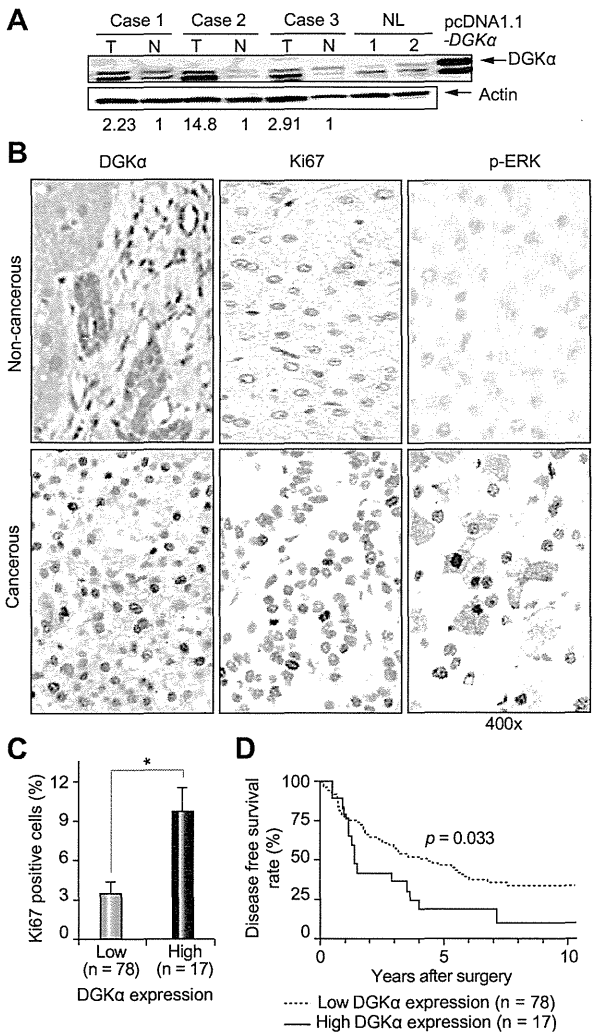

Fig. 4. DGKα expression in HCC samples. (A) DGKα expression in cancerous tissues (T), adjacent non-cancerous tissues (N) collected from surgical resection, and normal liver tissues (NL) was analyzed by Western blotting. DGKα expression levels were quantified by densitometry and normalized to β-actin. (B) DGKα, Ki67 and p-ERK expression in liver cancer samples was analyzed by immunohistochemistry. Normal bile duct cells indicated positive immunostaining for DGKα (400 × magnification). (C) Cell numbers positive for Ki67 are shown as mean ± S.D. Asterisks (*) indicate significant difference. (D) Disease-free survival curves after hepatectomy of the HCC patients comparing high and low DGKα expression.

A multivariate analysis of recurrence-free survival after hepatectomy was carried out using the Cox proportional hazards regression model. High DGKα expression was one of the independent risk factors for determining HCC recurrence after surgery ($p = 0.0184$; Table 2), as were intrahepatic metastasis ($p = 0.0004$), AFP >40 ng ($p = 0.0287$), and liver cirrhosis ($p = 0.0295$). The relative risk for HCC recurrence after hepatectomy in patients with high DGKα-expressing tumors was 2.32 times greater than that of patients with low DGKα-expressing tumors.

Table 2. Multivariate analysis of recurrence of HCC by Cox's proportional hazard model.

Factors	Odds ratio (95% CI)	*p* value
Intrahepatic metastasis		
Positive *vs.* negative	3.32 (1.75-6.10)	0.0004
DGKα		
High *vs.* low expression	2.32 (1.15-4.42)	0.0184
AFP >40 (ng/ml)	2.06 (1.07-3.89)	0.0287
Liver cirrhosis	1.92 (1.07-3.40)	0.0295

CI, confidence interval; DGKα, diacylglycerol kinase α; AFP, α-fetoprotein.

Discussion

Previous reports showed that DGKα enhanced interleukin 2-induced G1 to S transition and subsequent proliferation of T cells [18]. Another study reported that HGF induces DGKα activation in breast cancer cells, and is required for invasion [33]. Taken together, these findings imply that DGKα induces cell proliferation and invasion. Our findings have demonstrated the importance of DGKα as a potential tumor growth promoter in HCC. Furthermore, the inactive mutant, KD DGKα, failed to affect the extent of cell proliferation, thus, DG consumption or PA production might play an important role in the regulation of cell proliferation. It is known that the level of PA is also increased in cells transformed by oncogenes to promote proliferation [34,35]. As our study did not directly demonstrate DG consumption or PA production by DGKα in HCC, further studies are required to fully account for the mechanism as to how DGKα contributes to the progression of HCC. However, our results suggest that inhibition of DGKα or the catalytic activity could reduce HCC growth.

The therapeutic target for cancer should be the cancer-specific gene, whose upregulated or downregulated expression is limited to only cancerous cells, in order to enhance the effect of the therapy and to reduce side effects. In this study, DGKα expression was upregulated in HCC cell lines compared with normal hepatocytes, and was also increased in primary HCC tissue compared with adjacent non-tumor tissue *in vivo*. DGKα may be a novel target for HCC because of the specificity of HCC.

The MAPK signaling cascade is essential for the transduction of extracellular signals to the nucleus, regulating a wide variety of pathophysiological processes such as proliferation, differentiation, migration and carcinogenesis [36], and is the prominent pathway upregulated in HCC [37], making it an obvious target in the strategy for HCC treatment. This current study provides the first evidence that DGKα is a critical component in the MAPK pathway activated by HGF in HCC. Knockdown of DGKα impaired phosphorylation of ERK and of MEK, but not Ras activity. In addition, *DGKα* silencing activated Ras more strongly than the control, following 60 min of HGF stimulation. Ras was inactivated by ERK phosphorylation through negative feedback mechanisms [38]. These facts imply that the target component of DGKα might be Raf. We previously showed that DGKη activated the MAPK pathway induced by EGF, by augmenting the activity and heterodimerization of Raf in HeLa [39]. DGKα may contribute to activation of the MAPK pathway instead of Ras activation in HCC progression.

In conclusion, DGKα expressed in human HCC appears to have an important role in cell proliferation and invasion in HCC via

activation of the MAPK cascade, and may determine the degree of malignancy of HCC. Inhibition of DGKα might contribute to suppression of HCC growth, thus DGKα could be a novel target for HCC therapeutics as well as a prognostic marker.

Conflict of interest

The authors who have taken part in this study declared that they do not have anything to disclose regarding funding or conflict of interest with respect to this manuscript.

Supplementary data

Supplementary data associated with this article can be found, in the online version, at http://dx.doi.org/10.1016/j.jhep.2012.02.026.

References

[1] Kiyosawa K, Umemura T, Ichijo T, Matsumoto A, Yoshizawa K, Gad A, et al. Hepatocellular carcinoma: recent trends in Japan. Gastroenterology 2004;127:S17–S26.

[2] Parkin DM. Global cancer statistics in the year 2000. Lancet Oncol 2001;2:533–543.

[3] Taketomi A, Sanefuji K, Soejima Y, Yoshizumi T, Uhciyama H, Ikegami T, et al. Impact of des-gamma-carboxy prothrombin and tumor size on the recurrence of hepatocellular carcinoma after living donor liver transplantation. Transplantation 2009;87:531–537.

[4] Taketomi A, Kitagawa D, Itoh S, Harimoto N, Yamashita Y, Gion T, et al. Trends in morbidity and mortality after hepatic resection for hepatocellular carcinoma: an institute's experience with 625 patients. J Am Coll Surg 2007;204:580–587.

[5] Shirabe K, Kanematsu T, Matsumata T, Adachi E, Akazawa K, Sugimachi K. Factors linked to early recurrence of small hepatocellular carcinoma after hepatectomy: univariate and multivariate analyses. Hepatology 1991;14:802–805.

[6] Taketomi A, Fukuhara T, Morita K, Kayashima H, Ninomiya M, Yamashita Y, et al. Improved results of a surgical resection for the recurrence of hepatocellular carcinoma after living donor liver transplantation. Ann Surg Oncol 2010;17:2283–2289.

[7] Lai JP, Sandhu DS, Moser CD, Cazanave SC, Oseini AM, Shire AM, et al. Additive effect of apicidin and doxorubicin in sulfatase 1 expressing hepatocellular carcinoma in vitro and in vivo. J Hepatol 2009;50:1112–1121.

[8] Schmitz KJ, Wohlschlaeger J, Lang H, Sotiropoulos GC, Malago M, Steveling K, et al. Activation of the ERK and AKT signalling pathway predicts poor prognosis in hepatocellular carcinoma and ERK activation in cancer tissue is associated with hepatitis C virus infection. J Hepatol 2008;48:83–90.

[9] Grant S. Cotargeting survival signaling pathways in cancer. J Clin Invest 2008;118:3003–3006.

[10] Sakane F, Imai S-i, Kai M, Yasuda S, Kanoh H. Diacylglycerol kinases: why so many of them? Biochim Biophys Acta 2007;1771:793–806.

[11] Topham MK. Signaling roles of diacylglycerol kinases. J Cell Biochem 2006;97:474–484.

[12] Goto K, Hozumi Y, Kondo H. Diacylglycerol, phosphatidic acid, and the converting enzyme, diacylglycerol kinase, in the nucleus. Biochim Biophys Acta 2006;1761:535–541.

[13] van Blitterswijk WJ, Houssa B. Properties and functions of diacylglycerol kinases. Cell Signal 2000;12:595–605.

[14] Merida I, Avila-Flores A, Merino E. Diacylglycerol kinases: at the hub of cell signalling. Biochem J 2008;409:1–18.

[15] Sakane F, Yamada K, Kanoh H, Yokoyama C, Tanabe T. Porcine diacylglycerol kinase sequence has zinc finger and E–F hand motifs. Nature 1990;344:345–348.

[16] Jiang Y, Qian W, Hawes JW, Walsh JP. A domain with homology to neuronal calcium sensors is required for calcium-dependent activation of diacylglycerol kinase alpha. J Biol Chem 2000;275:34092–34099.

[17] Sakane F, Yamada K, Imai S, Kanoh H. Porcine 80-kDa diacylglycerol kinase is a calcium-binding and calcium/phospholipid-dependent enzyme and undergoes calcium-dependent translocation. J Biol Chem 1991;266:7096–7100.

[18] Flores I, Casaseca T, Martinez AC, Kanoh H, Merida I. Phosphatidic acid generation through interleukin 2 (IL-2)-induced alpha-diacylglycerol kinase activation is an essential step in IL-2-mediated lymphocyte proliferation. J Biol Chem 1996;271:10334–10340.

[19] Yamada K, Sakane F, Kanoh H. Immunoquantitation of 80 kDa diacylglycerol kinase in pig and human lymphocytes and several other cells. FEBS Lett 1989;244:402–406.

[20] Olenchock BA, Guo R, Carpenter JH, Jordan M, Topham MK, Koretzky GA, et al. Disruption of diacylglycerol metabolism impairs the induction of T cell anergy. Nat Immunol 2006;7:1174–1181.

[21] Zha Y, Marks R, Ho AW, Peterson AC, Janardhan S, Brown I, et al. T cell anergy is reversed by active Ras and is regulated by diacylglycerol kinase-alpha. Nat Immunol 2006;7:1166–1173.

[22] Kanoh H, Iwata T, Ono T, Suzuki T. Immunological characterization of sn-1,2-diacylglycerol and sn-2-monoacylglycerol kinase from pig brain. J Biol Chem 1986;261:5597–5602.

[23] Liver Cancer Study Group of Japan. The General Rules for the Clinical and Pathological Study of Primary Liver Cancer. 2nd English ed. Kanehara: Tokyo; 2003.

[24] Yamada K, Sakane F, Imai S, Tsushima S, Murakami T, Kanoh H. Regulatory role of diacylglycerol kinase gamma in macrophage differentiation of leukemia cells. Biochem Biophys Res Commun 2003;305:101–107.

[25] Itoh S, Taketomi A, Tanaka S, Harimoto N, Yamashita Y, Aishima S, et al. Role of growth factor receptor bound protein 7 in hepatocellular carcinoma. Mol Cancer Res 2007;5:667–673.

[26] Anegawa G, Kawanaka H, Yoshida D, Konishi K, Yamaguchi S, Kinjo N, et al. Defective endothelial nitric oxide synthase signaling is mediated by rho-kinase activation in rats with secondary biliary cirrhosis. Hepatology 2008;47:966–977.

[27] Sharma D, Wang J, Fu PP, Sharma S, Nagalingam A, Mells J, et al. Adiponectin antagonizes the oncogenic actions of leptin in hepatocellular carcinogenesis. Hepatology 2010;52:1713–1722.

[28] Nakabayashi H, Taketa K, Yamane T, Miyazaki M, Miyano K, Sato J. Phenotypical stability of a human hepatoma cell line, HuH-7, in long-term culture with chemically defined medium. Gann 1984;75:151–158.

[29] MacNab GM, Alexander JJ, Lecatsas G, Bey EM, Urbanowicz JM. Hepatitis B surface antigen produced by a human hepatoma cell line. Br J Cancer 1976;34:509–515.

[30] Baldanzi G, Mitola S, Cutrupi S, Filigheddu N, van Blitterswijk WJ, Sinigaglia F, et al. Activation of diacylglycerol kinase alpha is required for VEGF-induced angiogenic signaling in vitro. Oncogene 2004;23:4828–4838.

[31] Calvisi DF, Ladu S, Gorden A, Farina M, Conner EA, Lee JS, et al. Ubiquitous activation of Ras and Jak/Stat pathways in human HCC. Gastroenterology 2006;130:1117–1128.

[32] Scholzen T, Gerdes J. The Ki-67 protein: from the known and the unknown. J Cell Physiol 2000;182:311–322.

[33] Filigheddu N, Cutrupi S, Porporato PE, Riboni F, Baldanzi G, Chianale F, et al. Diacylglycerol kinase is required for HGF-induced invasiveness and anchorage-independent growth of MDA-MB-231 breast cancer cells. Anticancer Res 2007;27:1489–1492.

[34] Hurst-Kennedy J, Boyan BD, Schwartz Z. Lysophosphatidic acid signaling promotes proliferation, differentiation, and cell survival in rat growth plate chondrocytes. Biochim Biophys Acta 2009;1793:836–846.

[35] Sugimoto Y, Whitman M, Cantley LC, Erikson RL. Evidence that the *Rous sarcoma* virus transforming gene product phosphorylates phosphatidylinositol and diacylglycerol. Proc Natl Acad Sci U S A 1984;81:2117–2121.

[36] Marshall CJ. Specificity of receptor tyrosine kinase signaling: transient versus sustained extracellular signal-regulated kinase activation. Cell 1995;80:179–185.

[37] Saxena NK, Sharma D, Ding X, Lin S, Marra F, Merlin D, et al. Concomitant activation of the JAK/STAT, PI3K/AKT, and ERK signaling is involved in leptin-mediated promotion of invasion and migration of hepatocellular carcinoma cells. Cancer Res 2007;67:2497–2507.

[38] Cirit M, Wang CC, Haugh JM. Systematic quantification of negative feedback mechanisms in the extracellular signal-regulated kinase (ERK) signaling network. J Biol Chem 2010;285:36736–36744.

[39] Yasuda S, Kai M, Imai S, Takeishi K, Taketomi A, Toyota M, et al. Diacylglycerol kinase eta augments C-Raf activity and B-Raf/C-Raf heterodimerization. J Biol Chem 2009;284:29559–29570.

J Gastroenterol (2013) 48:777–778
DOI 10.1007/s00535-013-0800-7

LETTER TO THE EDITOR

Serum HBV RNA as a possible marker of HBV replication in the liver during nucleot(s)ide analogue therapy

Masayuki Kurosaki · Kaoru Tsuchiya · Hiroyuki Nakanishi · Jun Itakura · Namiki Izumi

Received: 5 March 2013 / Accepted: 5 March 2013 / Published online: 30 March 2013

We read with interest the article by Tsuge et al. [1] published in the recent issue of the Journal of Gastroenterology. Treatment with nucleot(s)ide analogue (NUC) strongly suppresses the replication of hepatitis B virus (HBV) leading to a high rate of serum HBV DNA negativity. However, the incidence of relapse after the cessation of NUCs is high. Criterion for safe discontinuation of NUC therapy after long term therapy is not established to date. In HBe antigen positive patients, seroconversion, HBV DNA negativity and consolidation therapy of >6 months may be a consensus criteria but 30–50 % of patients fulfilling this criteria experience a relapse. In HBe antigen negative patients, NUC therapy is generally recommended until HBs antigen becomes undetected. Tsuge et al. [1] measured serum HBV RNA plus DNA by real time PCR and showed that the serum HBV DNA + RNA titer following 3 months of NUC treatment was a significant predictor of early (within 24 weeks) HBV DNA rebound after discontinuation of NUC. The serum HBV DNA + RNA titer was also associated with ALT rebound in HBe antigen positive patients. The results of the study by Tsuge et al. indicate that serum HBV DNA + RNA titer may serve as predictor of relapse after discontinuation of NUC.

The high rate of relapse after discontinuation of NUC is due to the persistence of HBV replication in the liver even during the NUC therapy. The replicative intermediate form of HBV, covalently closed circular DNA (cccDNA), may not be eliminated by NUC therapy and serves as a template for viral pre-genomic messenger RNA [2]. This concept was proved by a study showing that quantification of intrahepatic HBV cccDNA had a high accuracy of predicting sustained virological response after NUC discontinuation [3]. Still, we need a non-invasive and clinically usable marker for the assessment of HBV replication in the liver during NUC therapy. The measurement of HBV core related antigen may be an alternative [4]. The rationale of measuring HBV RNA in serum was that immature HBV particles including HBV RNA are released from hepatocytes during NUC treatment under the circumstances that pre-genomic HBV RNA are transcribed from HBV cccDNA, packaged into HBV core particles, but not reverse transcribed into plus-strand HBV DNA due to strong interference by NUC, and the excessive amounts of these immature particles are accumulated in hepatocytes [5, 6]. Tsuge et al. showed that serum HBV DNA + RNA titer following 3 months of NUC treatment was significantly lower in patients with no rebound of HBV DNA. By using a cut-off value of 4.8 log copies/mL, the cumulative incidence of HBV DNA rebound was significantly lower in patients with serum HBV DNA + RNA titer < 4.8 log at 3 months of NUC treatment. The same groups previously showed that HBV RNA levels at 3 months of lamivudine treatment were predictor of early emergence of resistant mutations [7]. Taken together, serum HBV DNA + RNA titer may be linked to the level of HBV replication in the liver during NUC therapy. Monitoring of serum HBV DNA + RNA response may be utilized in various decision makings in treatment of HBV patients with NUC therapy.

Based on these important findings, several questions may remain for future elucidation. Commercially available transcription-mediated amplification and hybridization assay

An answer to this letter to the editor is available at doi:10.1007/s00535-013-0801-6.

M. Kurosaki (✉) · K. Tsuchiya · H. Nakanishi · J. Itakura · N. Izumi
Department of Gastroenterology and Hepatology, Musashino Red Cross Hospital, 1-26-1 Kyonan-cho, Musashino-shi, Tokyo 180-8610, Japan
e-mail: kurosaki@musashino.jrc.or.jp

(TMA) detects both HBV DNA and RNA. We do recognize that detection sensitivity of this assay is not sensitive but could this assay be used in alternative to real time PCR? In the present study, duration of therapy was 36 weeks in average. The question is whether serum HBV DNA + RNA decrease further by a longer duration of therapy and whether monitoring of serum HBV DNA + RNA (at the end of treatment) serve as a predictor of safe discontinuation after long term NUC therapy. Various protocols of sequential interferon therapy starting with NUC are reported in an attempt to enhance the antiviral activity or to achieve drug-free status [8]. However, their outcome varies considerably and negative HBe antigen at the start of interferon is the only predictor of response [9]. Since 26 out of 36 patients in the study by Tsuge et al. received sequential interferon therapy, serum HBV DNA + RNA titer may be an alternative predictor of favorable response to sequential interferon therapy. Further investigation may be necessary to solve these issues but readers of the journal may be interested if comments can be made by the authors.

Conflict of interest The authors declare that they have no conflict of interest.

References

1. Tsuge M, Murakami E, Imamura M, Abe H, Miki D, Hiraga N, et al. Serum HBV RNA and HBeAg are useful markers for the safe discontinuation of nucleotide analogue treatments in chronic hepatitis B patients. J Gastroenterol. 2013. Epub 2013/02/12.
2. Moraleda G, Saputelli J, Aldrich CE, Averett D, Condreay L, Mason WS. Lack of effect of antiviral therapy in nondividing hepatocyte cultures on the closed circular DNA of woodchuck hepatitis virus. J Virol. 1997;71(12):9392–9. Epub 1997/11/26.
3. Sung JJ, Wong ML, Bowden S, Liew CT, Hui AY, Wong VW, et al. Intrahepatic hepatitis B virus covalently closed circular DNA can be a predictor of sustained response to therapy. Gastroenterology. 2005;128(7):1890–7. Epub 2005/06/09.
4. Kimura T, Rokuhara A, Sakamoto Y, Yagi S, Tanaka E, Kiyosawa K, et al. Sensitive enzyme immunoassay for hepatitis B virus core-related antigens and their correlation to virus load. J Clin Microbiol. 2002;40(2):439–45. Epub 2002/02/05.
5. Su Q, Wang SF, Chang TE, Breitkreutz R, Hennig H, Takegoshi K, et al. Circulating hepatitis B virus nucleic acids in chronic infection: representation of differently polyadenylated viral transcripts during progression to nonreplicative stages. Clin Cancer Res. 2001;7(7):2005–15. Epub 2001/07/13.
6. Zhang W, Hacker HJ, Tokus M, Bock T, Schroder CH. Patterns of circulating hepatitis B virus serum nucleic acids during lamivudine therapy. J Med Virol. 2003;71(1):24–30. Epub 2003/07/15.
7. Hatakeyama T, Noguchi C, Hiraga N, Mori N, Tsuge M, Imamura M, et al. Serum HBV RNA is a predictor of early emergence of the YMDD mutant in patients treated with lamivudine. Hepatology. 2007;45(5):1179–86. Epub 2007/04/28.
8. Yokosuka O, Kurosaki M, Imazeki F, Arase Y, Tanaka Y, Chayama K, et al. Management of hepatitis B: consensus of the Japan Society of Hepatology 2009. Hepatol Res. 2011;41(1):1–21. Epub 2010/11/13.
9. Enomoto M, Nishiguchi S, Tamori A, Kobayashi S, Sakaguchi H, Shiomi S, et al. Entecavir and interferon-alpha sequential therapy in Japanese patients with hepatitis B e antigen-positive chronic hepatitis B. J Gastroenterol. 2012. (Epub 2012/08/02).

Hepatology Research

Hepatology Research 2013 doi: 10.1111/hepr.12254

Original Article

Hepatic oxidative stress in ovariectomized transgenic mice expressing the hepatitis C virus polyprotein is augmented through suppression of adenosine monophosphate-activated protein kinase/proliferator-activated receptor gamma co-activator 1 alpha signaling

Yasuyuki Tomiyama, Sohji Nishina, Yuichi Hara, Tomoya Kawase and Keisuke Hino

Department of Hepatology and Pancreatology, Kawasaki Medical School, Kurashiki, Japan

Aim: Oxidative stress plays an important role in hepatocarcinogenesis of hepatitis C virus (HCV)-related chronic liver diseases. Despite the evidence of an increased proportion of females among elderly patients with HCV-related hepatocellular carcinoma (HCC), it remains unknown whether HCV augments hepatic oxidative stress in postmenopausal women. The aim of this study was to determine whether oxidative stress was augmented in ovariectomized (OVX) transgenic mice expressing the HCV polyprotein and to investigate its underlying mechanisms.

Methods: OVX and sham-operated female transgenic mice expressing the HCV polyprotein and non-transgenic littermates were assessed for the production of reactive oxygen species (ROS), expression of inflammatory cytokines and antioxidant potential in the liver.

Results: Compared with OVX non-transgenic mice, OVX transgenic mice showed marked hepatic steatosis and ROS production without increased induction of inflammatory cytokines, but there was no increase in ROS-detoxifying enzymes such as superoxide dismutase 2 and glutathione peroxidase 1. In accordance with these results, OVX transgenic mice showed less activation of peroxisome proliferator-activated receptor-γ co-activator-1α (PGC-1α), which is required for the induction of ROS-detoxifying enzymes, and no activation of adenosine monophosphate-activated protein kinase-α (AMPKα), which regulates the activity of PGC-1α.

Conclusion: Our study demonstrated that hepatic oxidative stress was augmented in OVX transgenic mice expressing the HCV polyprotein by attenuation of antioxidant potential through inhibition of AMPK/PGC-1α signaling. These results may account in part for the mechanisms by which HCV-infected women are at high risk for HCC development when some period has passed after menopause.

Key words: antioxidant potential, glutathione peroxidase, reactive oxygen species, superoxide dismutase

INTRODUCTION

PERSISTENT HEPATITIS C virus (HCV) infection is a major risk factor for the development of hepatocellular carcinoma (HCC) in Japan. Approximately 70% of Japanese HCC patients are currently diagnosed with HCV-associated cirrhosis or chronic hepatitis C.[1] Nevertheless, the mechanisms underlying HCV-associated hepatocarcinogenesis are incompletely understood. Notably, there is sex disparity in HCC development, that is, male sex has been demonstrated to be an independent risk factor associated with HCC development.[2-4] It is proposed that estrogen-mediated inhibition of interleukin (IL)-6 production by Kupffer cells reduces the HCC risk in females.[5] In addition, the proportion of females among elderly patients with HCV-related HCC has recently increased in Japan.[6] These results suggest that menopause may be a risk factor associated with HCC development in female patients with HCV infection.

Numerous studies have shown that oxidative stress is present in chronic hepatitis C to a greater degree than in other inflammatory disease,[7,8] and is related to

Correspondence: Professor Keisuke Hino, Department of Hepatology and Pancreatology, Kawasaki Medical School, 577 Matsushima, Kurashiki, Okayama 701-0192, Japan. Email: khino@med.kawasaki-m.ac.jp

Received 9 September 2013; revision 24 September 2013; accepted 30 September 2013.

hepatocarcinogenesis in HCV-associated chronic liver diseases.[9,10] We have previously demonstrated that transgenic mice expressing the HCV polyprotein develop liver tumors including HCC, in connection with oxidative stress induced by HCV and iron overload.[11] Interestingly, such hepatocarcinogenesis was observed only in male transgenic mice, suggesting that females are resistant to oxidative stress in these transgenic mice. On the other hand, it is reported that ovariectomy increases nicotinamide adenine dinucleotide phosphate (NADPH) oxidase activity[12] and decreases mitochondrial-reduced glutathione levels in rats.[13] However, it remains unknown how HCV affects ovariectomy-induced oxidative stress. Investigation of this issue may provide a clue for understanding why the incidence of HCC increases in elderly postmenopausal women with HCV infection. The aim of this study was to determine whether HCV proteins amplify oxidative stress induced by ovariectomy and to investigate the mechanisms underlying this.

METHODS

Animals

CONTAINING THE FULL-LENGTH polyprotein-coding region under the control of the murine albumin promoter/enhancer, the transgene pAlbSVPA-HCV has been described in detail.[14,15] Of the four transgenic lineages with evidence of RNA transcription of the full-length HCV-N open reading frame (FL-N), the FL-N/35 lineage proved capable of breeding in large numbers. There is no inflammation in the transgenic liver.[15]

Experimental design

Female FL-N/35 transgenic mice and their normal female C57BL/6 littermates were anesthetized for surgery and underwent either a bilateral ovariectomy or sham operation at the age of 4–6 weeks. We studied ovariectomized (OVX) transgenic mice ($n = 5$), sham-operated transgenic mice ($n = 5$), OVX non-transgenic mice ($n = 5$) and sham-operated non-transgenic mice ($n = 5$). These mice were fed a normal rodent diet, bred, maintained, and killed by i.p. injection of 10% pentobarbital sodium preceded by 20-h fasting at the age of 24 weeks. All experimental protocols and animal maintenance procedures used in this study were approved by the Ethics Review Committee for Animal Experimentation of Kawasaki Medical School.

Histological procedures

A portion of liver tissue was immediately snap-frozen in liquid nitrogen for determination of the hepatic triglyceride concentration. The remaining liver tissue was fixed in 4% paraformaldehyde in phosphate-buffered saline and embedded in paraffin for histological analyses. Liver sections were stained with hematoxylin–eosin.

Serum leptin concentration

The serum leptin level was measured using a Rat Leptin Elisa kit (Morinaga Institute of Biological Science, Yokohama, Japan) according to the manufacturer's instructions.

Hepatic triglyceride content

Lipids were extracted from the homogenized liver tissue by the method of Bligh and Dyer.[16] The triglyceride level was measured with a TGE-test Wako kit (Wako Pure Chemicals, Tokyo, Japan), according to the manufacturer's instructions. Protein concentrations in liver were determined by the method of Lowry *et al.*,[17] using a DC protein assay kit (Bio-Rad Laboratories, Hercules, CA, USA).

In situ detection of reactive oxygen species (ROS)

In situ ROS production in the liver was assessed by staining with dihydroethidium, as described previously.[18] In the presence of ROS, dihydroethidium (Invitrogen, Carlsbad, CA, USA) is oxidized to ethidium bromide and stains nuclei bright red by intercalating with the DNA.[19] Fluorescence intensity was quantified using National Institutes of Health image analysis software for 3 randomly selected areas of digital images for each mouse.

Hepatic iron content

Hepatic iron content was measured by atomic absorption spectrometry, as described previously,[11] and expressed as micrograms Fe per gram of tissue (wet weight).

Derivatives of reactive oxygen metabolites (dROM) and biological antioxidant potential (BAP)

The levels of dROM and BAP were measured using a Free Radical Elective Evaluator (Wismerll, Tokyo, Japan), as described previously.[20] Measurement of dROM is based on the ability of the transition metal ions to catalyze the formation of alkoxy and peroxy radicals from hydroper-

oxides present in serum. The results are expressed in conventional units as Carrtelli units (U.CARR), where 1 U.CARR corresponds to 0.8 mg/L H_2O_2. Measurement of BAP is based on the ability of antioxidants to reduce ferric (F^{3+}) ions to ferrous (Fe^{2+}) ions.

RNA isolation and real-time reverse transcription polymerase chain reaction (RT–PCR)

Total RNA was isolated using an RNeasy mini kit (QIAGEN, Hilden, Germany) and reverse-transcribed into cDNA by using a Superscript III reverse transcription kit (Invitrogen). The PCR reactions were run in the ABI Prism 7700 sequence detection system (Applied Biosystems, Foster, CA, USA). The levels of mRNA were determined using cataloged primers (Applied Biosystems) for mice (tumor necrosis factor [TNF]-α, Mm00443258_m1; IL-1β, Mm00434228_m1; IL-6, Mm00446190_m1; HAMP [gene encoding hepcidin], Mm00519025_mL; superoxide dismutase 2 [SOD2], Mm01313000_m1; glutathione peroxidase 1 [GPx1], Mm00656767_g1; and sirtuin 3 [SIRT3], Mm00452131_m1). Expression of these genes was normalized to expression of glyceraldehyde 3-phosphate dehydrogenase mRNA (GAPDH, Mm99999915_g1).

Isolation of mitochondria and nuclear fraction

Mitochondrial extraction from liver tissue was performed using a Qproteome Mitochondrial Isolation kit (QIAGEN) according to the manufacturer's instructions. The nuclear fraction from liver tissue was prepared using a Nuclear Extraction kit (Panomics, Fremont, CA, USA) according to the manufacturer's instructions.

Immunoblotting

Liver lysates and the mitochondrial and nuclear fractions from liver were separated by sodium dodecylsulfate polyacrylamide gel electrophoresis. The proteins were transferred to polyvinylidene difluoride membranes (Millipore, Bradford, MA, USA), blocked overnight at 4°C with 5% skim milk and 0.1% Tween-20 in Tris-buffered saline, and subsequently incubated for 1 h at room temperature with goat antihuman SOD2 antibody (Santa Cruz Biotechnology, Santa Cruz, CA, USA), rabbit antihuman GPx1 antibody (Abcam, Cambridge, MA, USA), rabbit antihuman SIRT3 antibody (Abcam), rabbit antihuman peroxisome proliferator-activated receptor-γ co-activator-1α (PGC-1α) antibody (Abcam), rabbit antihuman adenosine monophosphate-activated protein kinase-α (AMPKα) antibody (Cell Signaling Technology, Boston, MA, USA), rabbit antihuman phospho-AMPKα (Thr172) antibody (Cell Signaling Technology), rabbit antihuman mitochondrial heat shock protein 70 antibody (HSP70; Thermo Scientific, Rockford, IL, USA), rabbit antihuman β-actin antibody (Cell Signaling Technology) or rabbit antimouse lamin B1 antibody (Abcam). The membranes were washed and incubated with horseradish peroxidase (HRP)-conjugated donkey antigoat immunoglobulin (Ig)G (Santa Cruz Biotechnology) or HRP-conjugated donkey antirabbit IgG (GE Healthcare Life Sciences, Pittsburgh, PA, USA).

Statistical analysis

Quantitative values are expressed as mean ± standard deviation. Two groups among multiple groups were compared by the rank-based Kruskal–Wallis ANOVA test followed by Scheffé's test. The statistical significance of correlation was determined by the use of simple regression analysis. $P < 0.05$ was considered to be significant.

RESULTS

Ovariectomy enhanced hepatic steatosis in FL-N/35 transgenic mice

AS CONFIRMATION OF successful ovariectomy-induced suppression of endogenous estrogen production, the uterine weight of OVX mice was significantly decreased compared with that of sham-operated mice (Table 1). Dietary intake, bodyweight, liver weight and serum leptin levels were significantly greater in OVX mice than in sham-operated mice regardless of whether they were transgenic or non-transgenic (Table 1). Interestingly, the serum alanine aminotransferase (ALT) level was significantly higher in OVX transgenic mice than in mice in the other three groups, but the levels were comparable in OVX non-transgenic and sham-operated non-transgenic mice (Table 1). To determine why OVX transgenic mice have a higher ALT level, we investigated the liver histology of the mice in the four groups (OVX transgenic, sham-operated transgenic, OVX non-transgenic and sham-operated non-transgenic mice). In contrast to the mild to moderate degree of hepatic steatosis noted in OVX non-transgenic mice and sham-operated transgenic mice, OVX transgenic mice developed severe hepatic steatosis (Fig. 1a) without infiltration of inflammatory mononuclear cells. Hepatic triglyceride content was measured to quantify the degree of steatosis. The triglyceride content was significantly greater in OVX transgenic mice than in mice in the other three groups (Fig. 1b), which was consistent with the

Table 1 Body, liver and uterus weight and serum biochemical parameters

Body, liver, and uterus weight and serum biochemical parameters	Non-transgenic		Transgenic	
	Sham-operated	OVX	Sham-operated	OVX
Bodyweight (g)	21.5 ± 1.2	30.7 ± 4.9*	27.7 ± 4.6	34.2 ± 3.8**
Liver weight (g)	0.86 ± 0.075	1.09 ± 0.236*	0.90 ± 0.102	1.18 ± 0.156**
Ratio of liver to bodyweight	0.038 ± 0.037	0.035 ± 0.003	0.031 ± 0.002	0.034 ± 0.006
Uterus weight (g)	0.08 ± 0.01	0.01 ± 0.02*	0.09 ± 0.01	0.01 ± 0.01**
Total dietary intake (g)	337 ± 24	429 ± 13*	368 ± 28	490 ± 31**
Serum glucose (mg/dL)	222.9 ± 110.0	275.1 ± 121.4	284.0 ± 84.1	259.7 ± 108.9
Serum ALT (IU/L)	15.5 ± 6.5	30.6 ± 38.1	21.8 ± 11.4	281.2 ± 165.1***
Serum triglyceride (mg/dL)	99.9 ± 9.7	78.9 ± 10.8	98.3 ± 11.4	89.7 ± 13.3
Serum leptin (ng/mL)	0.45 ± 0.14	1.31 ± 0.31*	0.65 ± 0.22	1.60 ± 0.28**

Data are mean ± standard deviation.
*$P < 0.05$ compared with sham-operated non-transgenic mice. **$P < 0.05$ compared with sham-operated transgenic mice. ***$P < 0.01$ compared with mice in the other three groups.
ALT, alanine aminotransferase; OVX, ovariectomized.

results for hepatic steatosis. Thus, the increase in the serum ALT level in the OVX transgenic mice was thought to reflect the hepatic steatosis.

Ovariectomy increased ROS and IL-6 production in the liver

Only OVX transgenic mice showed marked hepatic steatosis, regardless of the comparable diet intake and the ratio of liver to bodyweight of OVX non-transgenic mice (Table 1). We have previously demonstrated that iron-overloaded male FL-N/35 transgenic mice expressing the HCV polyprotein develop severe hepatic steatosis through increased ROS production.[11] Therefore, we examined whether ROS production was relevant to the marked hepatic steatosis observed in the OVX transgenic mice. Ovariectomy significantly increased ROS (super-

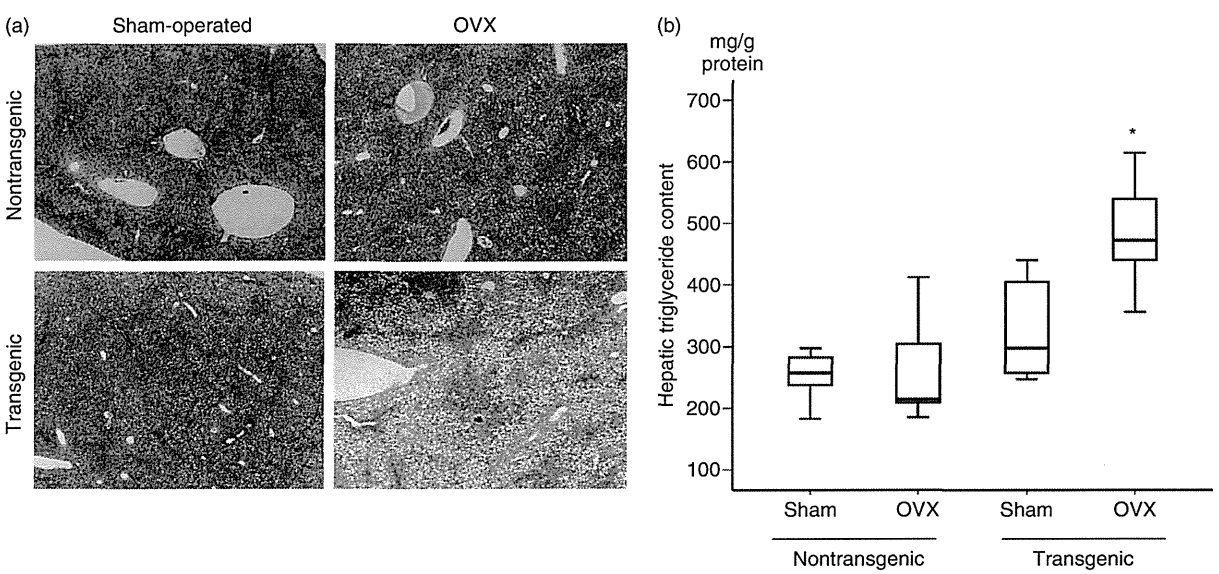

Figure 1 Hepatic steatosis and triglyceride content in sham-operated and ovariectomized (OVX) FL-N/35 transgenic and non-transgenic mice. (a) Hepatic steatosis in mice in each group (H&E, original magnification × 100). (b) Hepatic triglyceride content in mice in each group ($n = 5$). The results are shown as box plot profiles. The bottom and top edges of the boxes are the 25th and 75th percentiles, respectively. Median values are shown by the line within each box. *: $P < 0.05$ versus mice in the other three groups.

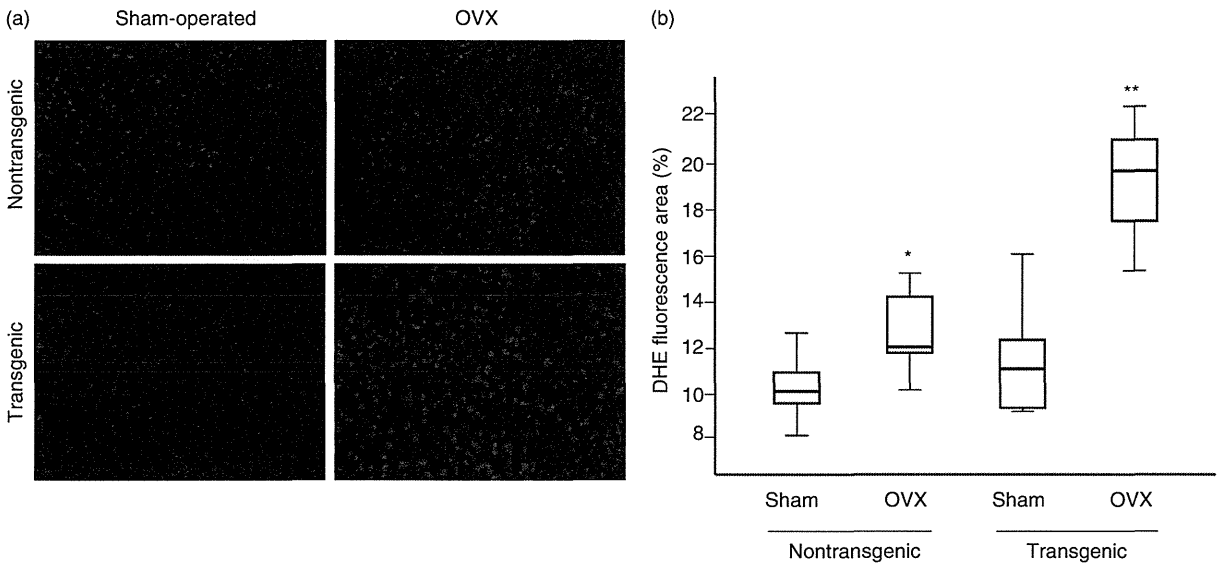

Figure 2 Reactive oxygen species (ROS) production in sham-operated and ovariectomized (OVX) FL-N/35 transgenic and non-transgenic mice. (a) Frozen liver sections from mice in each group were stained with dihydroethidium (DHE). (b) Fluorescence intensity was quantified by NIH image analysis software for three randomly selected areas of digital images for five mice in each group. The results are shown as box plot profiles. The bottom and top edges of the boxes are the 25th and 75th percentiles, respectively. Median values are shown by the line within each box. *: $P < 0.05$ versus sham-operated non-transgenic mice. **: $P < 0.05$ versus sham-operated nontransgenic mice, OVX non-transgenic mice and sham-operated transgenic mice.

oxide) production in both transgenic mice and non-transgenic mice, but the level of ROS production was greater in the OVX transgenic mice than in the OVX non-transgenic mice (Fig. 2). We next measured inflammatory cytokine levels in the liver. Ovariectomy significantly increased hepatic expression of IL-6 mRNA to the same degree in both transgenic mice and non-transgenic mice (Fig. 3). This ovariectomy-induced increase in hepatic IL-6 mRNA was consistent with the results of a previous report that OVX mice produced more hepatic

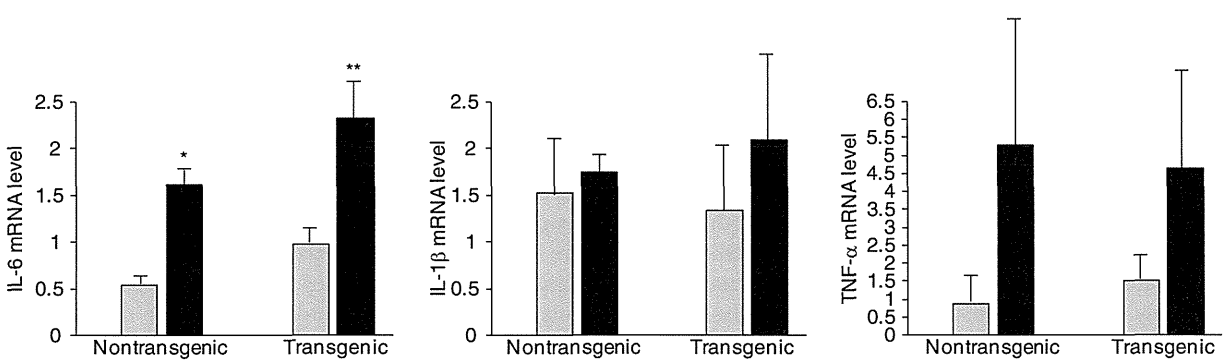

Figure 3 Expression levels of inflammatory cytokines in sham-operated and ovariectomized (OVX) FL-N/35 transgenic and non-transgenic mice. The mRNA levels of interleukin (IL)-6, IL-1β and tumor necrosis factor (TNF)-α were measured by real-time reverse transcription polymerase chain reaction for five mice in each group. The relative quantities of target mRNA in the liver were normalized with GAPDH mRNA. *$P < 0.05$ vs sham-operated non-transgenic mice. **$P < 0.05$ vs sham-operated transgenic mice. □, Sham; ■, OVX.

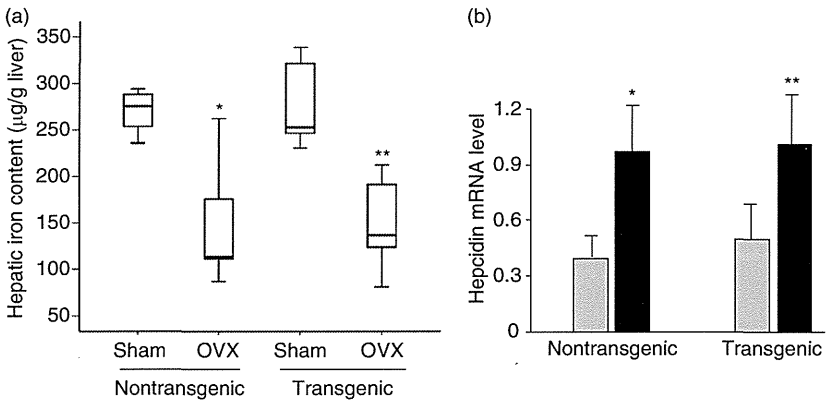

Figure 4 Hepatic iron content and hepcidin mRNA level in sham-operated and ovariectomized (OVX) FL-N/35 transgenic and non-transgenic mice. (a) Hepatic iron content in mice in each group ($n = 5$). The results are shown as box plot profiles. The bottom and top edges of the boxes are the 25th and 75th percentiles, respectively. Median values are shown by the line within each box. $^{*}P < 0.05$ vs sham-operated non-transgenic mice. $^{**}P < 0.05$ vs sham-operated transgenic mice. (b) The mRNA level of hepcidin was measured by real-time reverse transcription polymerase chain reaction for five mice in each group. The relative quantities of target mRNA in the liver were normalized with GAPDH mRNA. $^{*}P < 0.05$ vs sham-operated non-transgenic mice. $^{**}P < 0.05$ vs sham-operated transgenic mice. □, Sham; ■, OVX.

IL-6 than non-OVX mice after chemically induced liver injury.[5] There also was a trend for increase in TNF-α and IL-1β mRNA expression after ovariectomy in both the transgenic mice and non-transgenic mice, but their increases did not reach statistical significance, probably because of the large deviation (Fig. 3). These results suggested that inflammatory cytokines were unlikely to be associated with greater ROS production in OVX transgenic mice than in OVX non-transgenic mice.

Hepatic iron content and hepcidin expression level in the liver

We previously reported that male FL-N/35 transgenic mice developed hepatic iron accumulation through the reduced transcription of hepcidin,[18] a negative regulator in iron homeostasis.[21,22] Excess divalent iron can be highly toxic, mainly via the Fenton reaction producing hydroxyl radicals.[23] Therefore, we measured hepatic iron content to assess whether greater ROS production resulted from increased hepatic iron accumulation in OVX transgenic mice. Unexpectedly, ovariectomy significantly decreased hepatic iron content to the same degree in both transgenic mice and non-transgenic mice (Fig. 4a). These results are potentially explained by significantly increased transcription of hepcidin after ovariectomy (Fig. 4b). Ovariectomy-induced increase in hepatic IL-6 mRNA may in turn account for increased hepcidin transcription, because IL-6 acts to stimulate hepcidin expression through the STAT3 pathway.[24] These results suggested that hepatic iron content was not related to greater ROS production in OVX transgenic mice than in OVX non-transgenic mice.

Attenuated antioxidant potential against ovariectomy-induced ROS production in FL-N/35 transgenic mice

The increase in inflammatory cytokine production and the hepatic iron content after ovariectomy were comparable in transgenic and non-transgenic mice. Nevertheless, the serum ALT level, hepatic steatosis and ROS production were greater in OVX transgenic mice than in OVX non-transgenic mice. Therefore we measured dROM and BAP in serum to compare antioxidant potentials in OVX transgenic and OVX non-transgenic mice. We confirmed the significant negative correlation between the ratio of BAP to dROM and hepatic content of superoxide (Fig. 5). As expected, the values for dROM were higher in OVX mice than in sham-operated mice, regardless of whether they were transgenic or non-transgenic. However, a significant increase in the BAP value was found in OVX non-transgenic mice but not in OVX transgenic mice, which resulted in a lower ratio of BAP to dROM in the OVX transgenic mice than in the OVX non-transgenic mice (Table 2).

The first line of defense against ROS is the detoxifying enzymes that scavenge ROS. These include SOD and

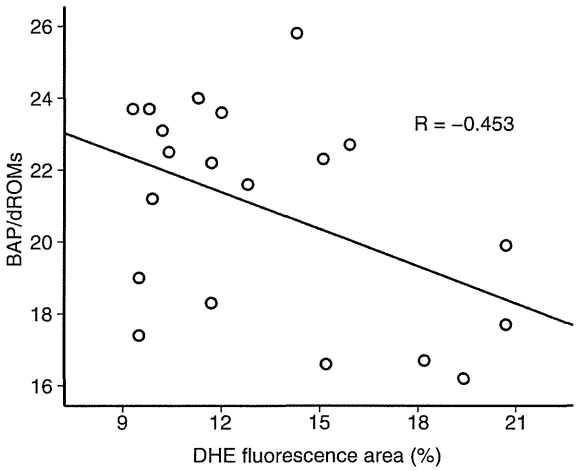

Figure 5 Negative correlation between the ratio of biological antioxidant potential (BAP) to derivatives of reactive oxygen metabolites (dROM) and hepatic content of superoxide. $R = -0.453$, $P < 0.05$. Hepatic content of superoxide was determined based on the area of dihydroethidium (DHE) fluorescence.

GPx1. Therefore we next investigated the expression levels of SOD2 and GPx1. The hepatic expression levels of SOD2 mRNA and GPx1 mRNA were significantly greater in OVX non-transgenic mice than in sham-operated non-transgenic mice, but were comparable in OVX transgenic mice and sham-operated transgenic mice (Fig. 6a). Western blot analysis of the hepatic mitochondria fractions also showed significant increases of SOD2 and GPx1 expression in OVX non-transgenic mice but not in OVX transgenic mice (Fig. 6b). These results suggested that antioxidant defense mechanisms may be induced against ovariectomy-related ROS production in non-transgenic mice but not in transgenic mice.

SIRT3 and PGC-1α expression in OVX FL-N/35 transgenic mice

Proliferator-activated receptor-γ co-activator-1α is a master regulator of mitochondrial biogenesis and respiration[25] and required for the induction of many ROS-detoxifying enzymes, including SOD2 and GPx1 upon oxidative stress.[26] SIRT3 is a member of a class III histone deacetylase and is reported to mediate PGC-1α-dependent induction of ROS-detoxifying enzymes.[27] In accordance with the changes in SOD2 and GPx1 levels after ovariectomy, the hepatic expression of SIRT3 mRNA was significantly greater in OVX non-transgenic mice than in sham-operated non-transgenic mice, but comparable in OVX transgenic mice and sham-operated transgenic mice (Fig. 7a). Western blot analysis of hepatic mitochondria showed a significant increase of SIRT3 expression in OVX non-transgenic mice but not in OVX transgenic mice (Fig. 7a).

Proliferator-activated receptor-γ co-activator-1α interacts with various nuclear receptors in addition to peroxisome proliferator-activated receptor-γ and is docked to the promoter of its target genes by all these nuclear receptors. Therefore, we investigated PGC-1α expression levels not only in liver homogenates but also in the nuclear fraction of mouse liver. The expression levels of PGC-1α in liver homogenates were comparable in sham-operated and OVX non-transgenic mice and in sham-operated and OVX transgenic mice. However, the expression levels of PGC-1α in the nuclear fraction of the liver significantly increased after ovariectomy in both non-transgenic and transgenic mice, and OVX transgenic mice had a lower PGC-1α expression level than OVX non-transgenic mice (Fig. 7b). These results suggested that the antioxidant potential against ovariectomy-induced ROS production may be reduced in OVX transgenic mice through lesser activation of PGC-1α than in OVX non-transgenic mice.

Table 2 Derivatives of reactive oxygen metabolites (dROM), biological antioxidant potential (BAP) and ratio of BAP to dROM

	Non-transgenic		Transgenic	
	Sham-operated	OVX	Sham-operated	OVX
dROM (U.CARR)	145.2 ± 15.1	158.7 ± 15.9*	170.8 ± 10.4	199.3 ± 21.1**
BAP (μmol/L)	3217 ± 123	3644 ± 177*	3362 ± 178	3542 ± 140
Ratio of BAP to dROM	22.3 ± 2.3	23.1 ± 2.0	20.8 ± 1.8	17.8 ± 1.9***

Data are mean ± standard deviation.
*$P < 0.05$ compared with sham-operated non-transgenic mice. **$P < 0.05$ compared with sham-operated transgenic mice. ***$P < 0.05$ compared with ovariectomized (OVX) non-transgenic mice.

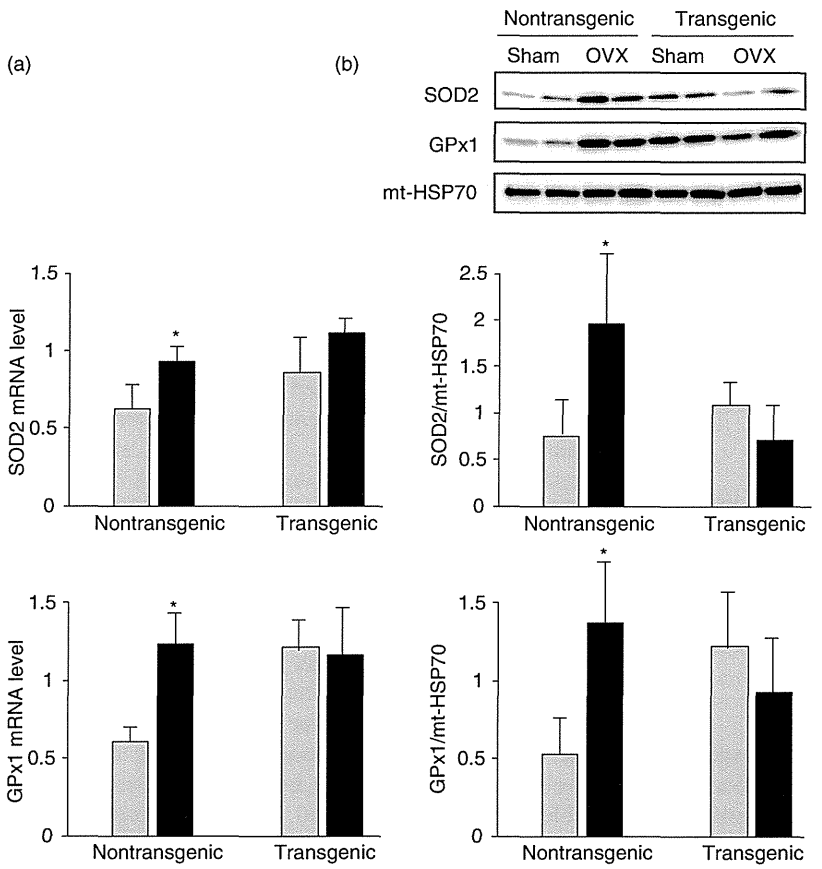

Figure 6 Expression levels of superoxide dismutase 2 (SOD2) and glutathione peroxidase 1 (GPx1) in sham-operated and ovariectomized (OVX) FL-N/35 transgenic and non-transgenic mice. (a) The mRNA levels of SOD2 and GPx1 were measured by real-time reverse transcription polymerase chain reaction for five mice in each group. The relative quantities of target mRNA in the liver were normalized with GAPDH mRNA. (b) Immunoblots for SOD2 and GPx1 were performed using mitochondrial fractions of liver lysates from five mice in each group. $^*P < 0.05$ vs sham-operated non-transgenic mice. □, Sham; ■, OVX.

Suppressed AMPK activation in OVX FL-N/35 transgenic mice

Proliferator-activated receptor-γ co-activator-1α activity is modulated through both transcriptional regulation and regulation of its activity by post-translational modifications.[28] AMPK is one of the signaling pathways regulating PGC-1α and acts both through modulation of PGC-1α transcription and by phosphorylation of the PGC-1α protein.[28] HCV has been shown to reduce the kinase activity of AMPK through Ser485/491 phosphorylation of AMPK.[29] Therefore, we examined the expression levels of AMPK to investigate the mechanisms underlying the lower PGC-1α expression in the nuclear fraction of the OVX transgenic liver. The expression levels of AMPKα, which is one of the three subunits (α, β and γ) of AMPK, were comparable in sham-operated and OVX mice and in non-transgenic and transgenic mice. However, the expression level of phosphorylated AMPKα was significantly greater in OVX non-transgenic mice than in mice in the three other groups, though it was similar in sham-operated transgenic mice and OVX transgenic mice (Fig. 7c). In addition, its levels were significantly greater in non-transgenic mice than in transgenic mice (Fig. 7c). These results suggested that AMPK was activated in OVX non-transgenic mice, but not in OVX transgenic mice, because AMPK is active only after phosphorylation of the α-subunit at a threonine residue within the kinase domain (T172) by upstream kinases.[30] Taken together, the results in the present study suggested that OVX FL-N/35 transgenic mice developed marked hepatic steatosis concomitant with increased ROS production via attenuation of antioxidant potential through inactivation of the AMPK/PGC-1α signaling pathway.

DISCUSSION

THE OVX MICE in the present study were assumed to be a standard model for evaluating the biological effect of ovariectomy because the effects of ovariectomy

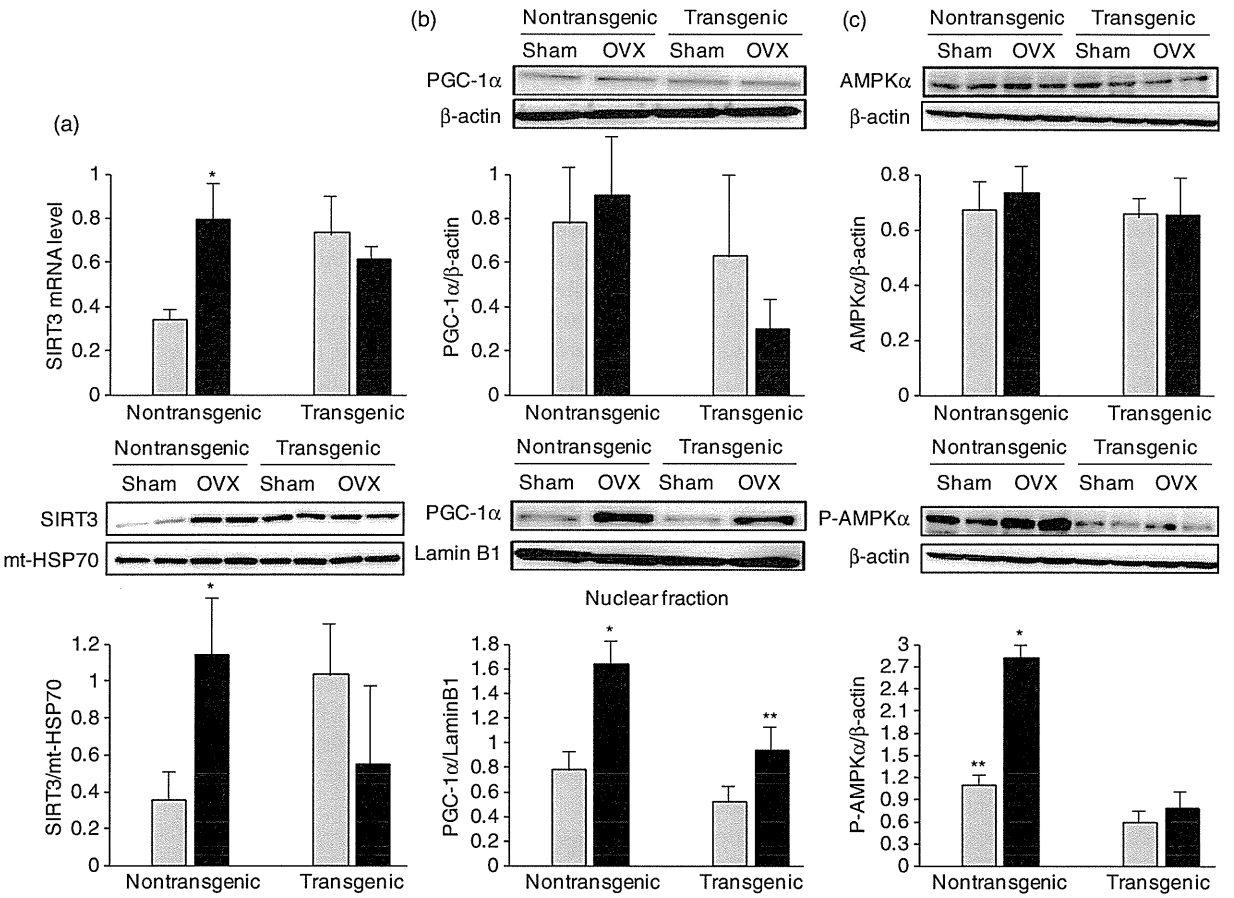

Figure 7 Expression levels of sirtuin 3 (SIRT3), peroxisome proliferator-activated receptor-γ co-activator-1α (PGC-1α), adenosine monophosphate-activated protein kinase α (AMPKα), and phosphorylated AMPKα (P-AMPKα) in sham-operated and ovariectomized (OVX) FL-N/35 transgenic and non-transgenic mice. (a) The mRNA levels of SIRT3 were measured by real-time reverse transcription polymerase chain reaction for five mice in each group. The relative quantities of target mRNA in the liver were normalized with GAPDH mRNA. Immunoblots for SIRT3 were performed using the mitochondrial fractions of liver lysates from five mice in each group. (b) Immunoblots for PGC-1α were performed using liver lysates and their nuclear fractions from five mice in each group. $*P < 0.05$ vs mice in the other three groups. $**P < 0.05$ vs sham-operated transgenic mice. (c) Immunoblots for AMPKα and P-AMPKα were performed using liver lysates from five mice in each group. $*P < 0.05$ vs mice in the other three groups. $**P < 0.05$ vs sham-operated transgenic mice. □, Sham; ■, OVX.

on dietary intake, bodyweight, uterine weight, liver weight and serum leptin levels were similar to the results from previous studies.[31–34] Ovariectomy increased ROS (superoxide) production in both transgenic liver and in non-transgenic liver, which was consistent with the ovariectomy-induced increase in NADPH oxidase activity[12] and the protective effect of estrogen against mitochondrial oxidative damage[13] found in previous studies. Of note was the much greater degree of ROS production after ovariectomy in transgenic mice than in non-transgenic mice. These results suggested that HCV protein expression has the potential to increase the sensitivity to oxidative stress in the liver. At least two possibilities may account for the increased sensitivity to oxidative stress in FL-N/35 transgenic mice. One possibility is an additive effect of HCV-induced ROS production on ovariectomy-induced oxidative stress. The HCV core protein has been shown to inhibit mitochondrial electron transport[35] and to induce ROS production.[36] In fact, basal ROS production tended to be higher in